THESIS

EVALUATION OF RAPID SCANNING TECHNIQUES FOR INSPECTING CONCRETE BRIDGE DECKS WITH ASPHALT OVERLAY

Submitted by

Sri Harsha Vemuri

Department of Civil and Environmental Engineering

In partial fulfillment of the requirements

For the Degree of Master of Science

Colorado State University

Fort Collins, Colorado

Spring 2016

Master's Committee:

Advisor: Rebecca Atadero

Suren Chen
Kelly Strong

ABSTRACT

EVALUATION OF RAPID SCANNING TECHNIQUES FOR INSPECTING CONCRETE BRIDGE DECKS WITH ASPHALT OVERLAY

The average age of bridges in the USA is 42 years. The life expectancy of a majority of these bridges is 50 years. At the current rates of aging and replacement, almost half of the nation's bridges will require major structural investment in the next 15 years as stated by the Federal Highway Administration. There is a severe deficiency in both time and resources available to address this problem, and methods to increase efficiency are needed. Bridge decks are the most critical elements of a bridge structure as they are directly and continuously exposed to harsh weather conditions and cyclic loading from traffic throughout their lifespan. This thesis attempts to improve management practices for bridge decks by addressing current challenges faced by the Colorado Department of Transportation (CDOT) in estimating the extent of damage on bridge decks.

The current bridge deck inspection method being employed by CDOT is sounding and chipping. This procedure involves sounding the deck with chains, hammers and rotary percussion to detect the deteriorated areas followed by chipping. The issues with this procedure include its time-consuming nature, the requirement for traffic to be diverted for extended periods and the costs associated with the inspection and traffic diversion. Additionally, sounding is not adequate to provide a rough estimation of the class of damaged area and the resulting expenses. CDOT wants to take the advantage of newer alternative techniques to evaluate bridge decks.

The alternative evaluation considered by CDOT involves using Ground Penetrating Radar (GPR) and Infrared Thermography (IR) thermography together for evaluating bridge decks. The major advantage of using GPR is that it is the only available method that can estimate the deterioration in concrete decks with asphalt overlay. Additionally, GPR can estimate the deterioration in early stages, unlike sounding which detects damage in advanced stages and GPR is also capable of detecting corrosion in rebars. Thus, GPR not only has the potential to address the disadvantages of sounding it also has additional advantages which can benefit the life of the bridge deck. This study attempts to understand the limitations that this newer evaluation method comes with and possibly solve some of these limitations to take complete advantage of this technology. This study took advantage of the available as-built data of four bridge decks rebuilt after sounding and chipping and the data available from GPR and IR scanning of the respective decks to study the limitations from using GPR and IR technologies.

The scanned results from GPR and IR thermography are compared to the deck condition data from sounding and chipping. In two cases the damage detected by GPR and IR thermography did not correlate well with the damage detected from sounding and chipping.

The two decks with reasonable correlation are compared to the decks with poor correlation in an effort to understand the possible causes for deviation in results. It was observed that for the decks with poor correlation the GPR showed areas with higher cover as deteriorated in the estimation. An improved data processing procedure to solve such miss-interpretation issue is suggested, and a coring strategy to assist future research in the direction of eliminating the depth-amplitude effects in GPR scans.

ACKNOWLEDGEMENT

The author would like to place his sincere thanks to his advisor Dr. Rebecca Atadero for her support, guidance and mentorship throughout his graduate course work and thesis. He would like to thank Dr. Suren Chen for his instruction in bridge engineering and for being a part of this thesis committee. He would also like to place his gratitude towards Dr. Kelly Strong for providing his insight in this work and being a part of this thesis committee.

The author would like to place his gratitude towards John Deland, Randy Wampler, Adam Carmichael, Ken Maser, Infrasense, inc., TSH engineering and CDOT for their continued support, insight, and their valuable time towards this work.

Without the support of the aforementioned, this thesis would not have been possible. Thank you.

TABLE OF CONTENTS

LIST OF TABLES

LIST OF FIGURES

1. INTRODUCTION

1.1 Motivation

The 2013 Report Card for America's Infrastructure by the American Society of Civil Engineers (ASCE) states that the average age of the bridges in the USA is 42 years. A third of the nation's bridge deck area is structurally deficient (ASCE, 2013). The Federal Highway Administration estimates that to eliminate the backlog by the year 2028 the nation needs to spend $20.5 billion per annum, which is $8 billion dollars more than what is currently being spent (ASCE, 2013). The national goal as of today is to reduce the number of deficient bridges to 8% by the year 2020 (ASCE, 2013). This means along with a deficit in budget allocation for bridge rehabilitation there is also a time constraint under which the nation has to work, emphasizing the importance of implementing an efficient strategy on both grounds.

Bridge inspection plays a pivotal role to make any sort of judgments related to the status of a bridge or the rehabilitation requirements. Missing critical defects during inspections could result in fatal consequences such as the case of Silver Bridge in Point Pleasant (Huston, Hu, Pelczarski, & Esser, 1999) West Virginia. In this case, a bridge collapsed due to a cleavage fracture caused by a critical-size flaw that developed over the 40-year life of the structure due to combined action of corrosion fatigue and stress corrosion. The collapse of 1460 feet long suspended section of the bridge claimed 46 victims and 32 vehicles and an estimated loss of 1 million dollars a month until restoration. In the US, bridge inspections are required to be made at least once every 24 months (AASHTO, 2011). AASHTO (American Association of State and Highway Transportation) suggests an approach in which a bridge is discretized into commonly

recognized structural elements such as Decks, Railings, Superstructure, Bearings, Substructure, etc., (AASHTO, 2013).

One of the more vulnerable bridge elements is the bridge deck. Decks are directly exposed to harsh environmental conditions and are subjected to cyclic loading all the time. Bridge owners often make their decisions whether to make a major rehabilitation or superficial maintenance based on the state of the bridge deck. In a way, the bridge deck acts as a barometer to indicate the performance of the bridge (Tonias, 1995)

Finding the right technique to inspect bridge decks is very important because failure to evaluate such element level conditions and implement corrective measures could lead to a reduction in loading capacity of the structure and even failure in extreme cases. Bridge deck maintenance constitutes 50-80% of all expenditures related to bridge inspection hence deck inspection reports of higher accuracy allow the engineers to make decisions with more efficiency (Gucunski, et al., 2011).

Over the past few decades, non-destructive evaluation (NDE) techniques have been developed and put into execution for faster and more effective inspection of bridge elements. The implementation of NDE techniques has impacted the time required for detection, analysis and diagnosis of various structural problems. Some of the NDE techniques are complicated and require trained personnel to gather, process and analyze the data (Lee & Kalos, 2014). Hence, the NDE tests selected by the decision-making parties are selected based on the anticipated types of defects, reliability, complexity, time available and availability of trained personnel.

The Colorado Department of Transportation (CDOT) pays contractors for a unit area of deck removal for repair based on the class of the deck removal. Following are the three classes of deck removal as stated by CDOT.

Class-1: Class-1 involves removal of spalling concrete on the surface to a depth not less than ¾” until the removal reaches sound concrete. In case the sound concrete is deeper than the centerline of the mat of top reinforcement then class 2 removal is required. Class 1 removal includes the removal of deck concrete and the overlay of a rigid deck. For other types of overlays (e.g. asphalt) the costs for removal of the overlay is added to concrete removal costs.

Class-2: Class-2 involves removal of concrete deck extending to the sound concrete. The removal has to extend to a minimum depth of 1 in. below the top longitudinal and transverse reinforcement steel. Whenever the concrete is lacking bond with surrounding reinforcement or when class-1 removals extend beyond the centerline of rebars the removals are continued up to minimum class-2 depths. The removal shall not go deeper than the top of bottom reinforcement mat. In case the sound concrete is not reached before the top of bottom reinforcement mat then class-3 removal is required.

Class-3: Class-3 removals extend to the full depth of concrete decks. The major challenges in bridge deck inspection as reported by the CDOT (Colorado Department of Transportation) are the absence of a reliable evaluation method to estimate the repair quantities for each class of removal and the lane closures that the transportation authorities have to enforce to execute the time-consuming inspection procedures. Addressing these problems will help CDOT to plan and spend its resources in a more efficient way.

CDOT is looking into alternative methods of evaluation that are more accurate in quantity estimation and use lesser resources. A newer alternative method that CDOT is considering involves using GPR (Ground Penetrating Radar) in combination with IR (Infrared Thermography). The major advantage of this technology is that it is the only available rapid scanning technology available to evaluate concrete bridge decks with asphalt overlays. There is

a need to understand and address the limitations that GPR and IR thermography could come with for evaluating concrete bridge decks.

1.2 Research Objectives

The overall goal of this research is to help CDOT take advantage of using new technology that involves GPR and IR to evaluate bridge decks by understanding their limitations and possibly address its limitations. This thesis attempts to achieve this goal through the following specific objectives.

The primary objective is to understand and improve the accuracy of estimations made using GPR and IR. Using the accuracy of these results the research attempts to find and study areas on the deck that are constantly deviating from the actual condition. Doing so, this study attempts to suggest areas of constant inaccuracy and alternative techniques that can be used to evaluate such areas and the impact of adapting to newer evaluation techniques from the traditional methods.

The secondary objective of this research is to put forward questions and suggestions for future study. Doing so, this study attempts to contribute to the progress in this technology.

2. BACKGROUND

2.1 Concrete Bridge Deck Deterioration

The causes of bridge deck deterioration can be chemical, physical or biological in nature. The distresses in bridge decks are a result of either corrosion in reinforcing steel or deterioration in concrete. The concrete deterioration and rebar corrosion are interrelated with one usually resulting from the other and ultimately affecting the integrity of the structure (Gucunski, et al., 2013). According to the manual for bridge inspections, the defects that can be identified in deck inspection are classified into Delamination/Spalls/Patched Area, Exposed Rebar, Efflorescence/Rust staining, Cracking, Abrasion/Wear and Damage (AASHTO, 2013).

2.1.1 Rebar Corrosion

Concrete bridge decks consist of concrete and reinforcing steel, of the two concrete and reinforcing steel the reinforcing steel is the more vulnerable element of a bridge deck. The limiting factor to the expectancy of a bridge deck is greatly dependent on reinforcement corrosion (Rhazi, 2011). The direct result of Corrosion is a loss of steel and rust. The volume of the resulting rust is 3 to 4 times more the original volume resulting in internal stresses in the sections of a deck and the subsequent Cracking, Delamination and Spalling (Nawy, 2008).

Corrosion in reinforcement is caused by the steel reinforcement acting as an electric cell due to the difference in the electric potential at two different areas of a steel rebar. The reinforcing steel is protected by the high alkaline nature of cement-based elements in concrete. The abundance of Hydroxide Ions along with steel reinforcement helps form Ferric Hydroxide, which forms a protective a layer of oxide over the steel reinforcement. Sufficient amount of concrete can act as a satisfactory protection. This protective layer of oxide can exist only exist

the concrete is at a pH value over 9.5. The rebars corrode when the pH value is below 9.5 or when the protective oxide layer is destroyed (Gucunski, Romero, Kruschwitz, Feldmann, & Parvardeh, 2011). Equations (1) and (2) are anodic and cathodic reactions that cause corrosion in steel bars.

Anodic reaction: $Fe \rightarrow Fe^{2+} + 2e^-$ (1)

Cathodic reaction: $O_2 + 2H_2O + 2e^- \rightarrow 4OH^-$ (2)

The traditional sounding technique used by CDOT cannot detect corroded bars in the deck. At the time of deck removal corrosion is taken care of by removing the steel bars that have lost more than half of their sections due to corrosion. These steel bars are replaced with newer ones. Sacrificial anodes are installed to stop the progression of corrosion in the deck. But this method does not necessarily detect all the corroded steel that could have lost considerable sections from corrosion. Which is necessary to protect the structural integrity of the deck.

Corrosion can result from various phenomenon all of which lead to formation of anodic areas in the reinforcement some of the common causes of corrosion are discussed in the following subsections.

2.1.1.1 Corrosion from Chloride Ions

Typically corrosion in steel reinforcement is initiated by chloride ion penetration. When the chloride ions penetrate into decks and settle on the steel rebars this area of the rebar acts as an area of negative potential (Anode), the other regions of reinforcement unaffected by chlorides are now at a relatively higher potential causing them to act as cathodes. This formation of areas of negative and positive potential can lead to the formation of an electric cell when current flows from areas of lower potential to higher potential. The electric cell formed due to the current flowing from top reinforcement anodic areas to the cathodic areas of reinforcement bars at the

bottom is known as macro-cell. In a similar interaction between two areas of the same rebar forms a cell this type of cell is known as a microcell. The resulting iron from the anodes goes into the solution destroying the rebars, once initiated corrosion process is continuous and active process whenever there is a presence of oxygen and moisture. In the resulting heterogeneous cross-section from corrosion only the sound steel is effective in carrying stresses (Gucunski, Romero, Kruschwitz, Feldmann, & Parvardeh, 2011).

Chloride action can be initiated from the atmospheric conditions or when dissolved salts form Chloride Ions. For instance, when salts such as Sodium Chloride dissolve in water they form a solution of sodium and chloride Ions, these active Chloride Ions when they reach the rebars can initiate the corrosion process. Corrosion from chloride Ions attacking the reinforcement does not necessarily need the presence of salts in the atmosphere but the presence of salts can greatly accelerate the corrosion process. The presence of sulfate Ions has an equally damaging effect on concrete but this is a less common occurrence. Engineers traditionally consider Sulphate Ion penetration as a problem associated with the Industrial environment, Substructure and maritime locations (Vittery & Pearson-Kirk, 2008).

2.1.1.2 Carbonation

Carbonation is a slower occurrence than other corrosive processes, which makes the concrete lose its passivity due to continuous exposure to carbon dioxide in the atmosphere. This process occurs continuously through the design period of concrete making the concrete lose its alkalinity slowly through the entire depth, when this causes the concrete above the reinforcement to reach a pH value of 7 or less the reinforcement loses protection from concrete. Protection to reinforcement from carbonation is directly related to the depth of cover. Hence, the concrete decks designed for longer periods are provided with a greater cover. Carbonation process

accelerates when there is a higher concentration of Carbon dioxide in the atmosphere (Sagues, Moreno, Morris, & Andrade, 1997).

2.1.2 Efflorescence

Efflorescence results from the vaporization of water present in the pore structure of the concrete. Efflorescence could be classified as either primary or secondary efflorescence. The primary efflorescence occurs at the time of construction from the mixing of water. The secondary efflorescence is the efflorescence that forms after a construction usually from the vaporization of water present in the pores and joints. (Gucunski, Romero, Kruschwitz, Feldmann, & Parvardeh, 2011).

While the presence of efflorescence does not cause a loss in mechanical properties or durability of the structure but the salt accumulation can result in scaling and spalling along the pore space of the concrete. This process can lead to the exposure of rebar or formation of cracks in both the cases the rebar loses protection leading to corrosion (Gucunski, Romero, Kruschwitz, Feldmann, & Parvardeh, 2011).

2.1.3 Delamination in Concrete

Delamination in concrete is formation of horizontal cracking. Delamination of a concrete deck as mentioned earlier occur due to the internal stresses generated by higher volume of rebar cross section resulting from corrosion or due to cyclic loading from traffic. Delaminations can be local or in some cases extend throughout the deck area. They can occur in multiple planes between the steel reinforcement and the deck surface. Delaminations cannot be detected by visual inspections however when they are not repaired in time they progress to become open

spalls exposing the reinforcement. Hence not detecting delaminations on time can result in faster deterioration of the structure (Gucunski, et al., 2013).

Sounding is an effective technique to detect delaminations at later stages. The newer techniques such as GPR, IR, and Half-cell potential are capable of detecting delaminations at early stages. Detecting the delaminations at early stages helps in increasing the structure's life and reducing the maintenance costs in the future. Hence, it is important to adapt evaluation techniques that detect the delaminations at earlier stages.

2.1.4 Spalling in Concrete

Spalling can be described as pitting or flaking in concrete. Spalling in concrete can occur due to the resulting stresses from poor construction techniques or from environmental conditions. Spalling has no immediate impact on the mechanical properties of the deck. When spalling results in rebar exposure, it could proceed to rebar corrosion eventually affecting the structural integrity (Gucunski, Romero, Kruschwitz, Feldmann, & Parvardeh, 2011).

In circumstances when the rebars are not exposed spalling is still detrimental to the structure because concrete cover reduction over rebars makes the rebars more vulnerable to actions such as chloride penetration or carbonation. When a structure is designed for a life of 50 years with a minimum concrete cover of 20 mm, a loss of 2 mm in the cover reduces the expectancy of the structure by 20 years (Gucunski, Romero, Kruschwitz, Feldmann, & Parvardeh, 2011).

2.1.5 Vertical Cracking in Concrete

Apart from corrosion cracking in concrete can occur due to various other factors. Factors such as hydration heat, plastic shrinkage, changes to exterior temperatures, setting of

fresh concrete, cyclic loading from traffic, geometrical constraints placed when curing the concrete, freeze-thaw cycles etc. the resulting cracks worsen when the reinforcement corrosion takes place eventually (Gucunski, et al., 2013).

2.1.6 Assessment of Common Distresses

Listed in table 1 are commonly occurring distresses and the assessment methods that can be used to identify the distresses. The standard procedures for each of the Condition assessment methods as suggested by ASTM International and AASHTO can be identified using tables in **Error! Reference source not found.** A.

Table 1: Distresses and condition assessment methods (AASHTO, 2011)

Distress	**Condition assessment method**
Air pockets and Honeycombing	Chain Dragging, Coring, Ground Penetrating Radar, Hammer Sounding, Impact Echo, Ultrasonics, Visual Inspection.
Alkali-Silica Reaction	Coring, Petrographic Analysis, Visual Inspection
Carbonation	Coring, Penetration Dyes, Petrographic Analysis
Chloride Induced Corrosion	Chloride Concentration Testing, Coring, Half-Cell Potential, Rigid Chloride Permeability, Resistivity
Cracking	Impact-Echo, Penetration Dyes, Ultrasonics, Visual Inspection
Delamination	Chain Dragging, Coring, Ground Penetrating Radar, Hammer Sounding, Impact Echo, Infrared thermography, Ultrasonics
Polishing	Skid resistance testing
Potholing	Visual inspection
Scaling	Visual inspection
Spalling	Visual inspection
Surface Attack	Coring, Petrographic Analysis

2.2 Inspection Methods for Concrete Bridge Decks

Decks are traditionally inspected visually followed by methods such as hammering and chain drag. These inspections possess certain limitations; some of the major limitations are listed in table 2. Whenever subsurface condition of bridge decks is required, the data is obtained using the sample-coring method (Lau, 1991).

Table 2: Traditional methods and their limitations

Inspection method	**Limitations**	**References**
Visual Inspection	• The deterioration could be in advanced stage if it can be visually detected	(Vilbig & Allen, 2014)
Chain drag	• Method should not be used on Asphalt covered surfaces • Laborious and slow • Results are affected by external conditions such as weather and noise	(Scheff & Chen, 2000)
Hammering	• Slow and Labor-intensive • Estimations show a deviation of about 40%	(Vilbig & Allen, 2014)
Destructive Methods (Sample Coring, Saw-cutting Deconstruction)	• Laborious and time consuming • Destructive analysis • Representative only for the location at which core is taken from	(Lau, 1991)

There are a number of nondestructive tests that can be used to detect the distresses in a bridge deck. Based on the testing principle involved these tests can generally be classified under certain categories. Each of these methodologies uses a certain physical phenomenon such as strength, acoustics, thermal conductivity etc., and is capable of detecting certain distresses in bridge decks. Table 3 lists the categories of such physical phenomenon and the defects each one is capable of detecting (AASHTO, 2011).

Table 3: NDT methods and corresponding anomalies (AASHTO, 2011)

Methodology	**Defects**					
	Cracking	**Scaling**	**Corrosion**	**Wear and abrasion**	**Chemical attack**	**Voids in grout**
Strength	N	N	P	N	P	N
Sonic	F	N	G[b]	N	N	N
Ultrasonic	G	N	F	N	P	N
Magnetic	N	N	F	N	N	N
Electrical	N	N	G	N	N	N
Nuclear	N	N	F	N	N	N
Thermography	N	G[b]	G[c]	N	N	N
Radar	N	G[b]	G[c]	N	N	N
Radiography	F	N	F	N	N	F
Visual inspection	G	G	N	G	F	N

G = Good, F = Fair, P = Poor, N = Not suitable,
b = Beneath bituminous surfacing's,
c = Detects delaminations

It is important to note that no single test is capable of identifying all the types of distresses. For example delaminations can be detected using tests such as impact echo, chain dragging, hammering, ground penetrating radar or infrared thermography but to identify corrosion in rebars tests such as half-cell potential, ground penetrating radar or galvanic cell has to be used. Defects such as vertical cracks can be identified using only surface wave testing. The condition assessment techniques are selected based on the type of the distresses that need to be assessed, the availability of resources and the level of detail required.

Engineers can use the standard guidelines suggested by ASTM International, the American Association of State Highway and Transportation Officials (AASHTO) and the Strategic Highway Research Program (SHRP) to perform these tests.

2.3 Description of Techniques

2.3.1 Traditional methods

In the past, the state of bridge decks was evaluated through visual inspections supplemented with physical testing methods and coring. Some of these commonly used traditional methods are explained in the following sections.

2.3.1.1 Visual Inspections

Visual inspection is the most direct method of inspection. Traditionally this method is used to locate distresses such as cracks, spalling, efflorescence, discoloration in concrete, scaling etc. A common practice when a bridge is evaluated through visual inspection is to use hammering at the time of inspection. The inspector listens to the noise from hammering different sections of the bridge. When the outcome is a hollow sound it is indicative of damage at the section. When this method is practiced it is common for the inspector to underestimate the deterioration by 40% (Vilbig & Allen, 2014).

When the inspector is looking for cracks it is important to record the direction, location and approximate width of cracks. Having such records helps the inspector to understand the severity and possible cause of the cracking. Table 4 lists the common types of cracking and possible causes of each type of cracking. Knowing the cause of a cracking would help the owners of the bridge to take preventive measures to protect the deck of similar cracks in the future.

Table 4: Common types of cracking in bridge decks and possible causes (Mark Moore, 2000)

Cracking type	**Description**	**Possible causes**
Cracking in concrete decks without asphalt-overlay		
Transverse cracking	Cracking perpendicular to centerline	- Loading - Thermal and moisture - Gradient drying shrinkage
Longitudinal cracking	Cracking parallel to centerline	- Improper construction of longitudinal joints - Heavy load repetitions - Thermal and moisture gradients - Improper design of reinforcement
Joint Spalling	Cracking along joints	- Loss in elevation along joint or crack - Accumulation of loose material under the slab
Mid Slab Spalling	Cracking, fraying or chipping along slab edges	- Excessive stress at joints from debris in joints and subsequent expansion, freezing and thawing, Traffic loading - Poor design of load transfer
Joint Seal failure	Tearing of sealant/ Loss in adhesion	- Permanent compression in sealant
Pumping	Pumping or ejection through cracks	- Cracking and subsequent water infiltration
Cracking in Concrete decks with asphalt-overlay		
Reflective cracking	Cracking along edges of underlying slabs	- Movement in underlying slabs

Even though visual inspection method is a direct method when a distress can be visually recognized it could mean that the distress is in an advanced stage, detecting a distress at an early stage is safer and can save more resources spent on the rehabilitation (Vilbig & Allen, 2014). The reliability of the report on a deck's state from visual inspections is based upon the interpretation skill of the inspector.

Irrespective of the limitations visual inspections are mandatory because no single NDE method is capable of detecting all the types of distresses in a deck (Gucunski, et al., 2013).

Hence visual inspections are very important for preliminary inspections and decision-making on the NDE methods to use.

2.3.1.2 Coring

Initially coring and saw cutting were the only available procedures to obtain the subsurface conditions of the deck. Some conclusions can be drawn from a core sample just by looking at it. When a detailed evaluation is required the samples can be sent to the laboratory for more tests such as compressive strength, air content, freeze-thaw chloride determination etc. The test results from coring are accurate for the location from which the sample is obtained. (Lau, 1991).

Apart from the fact that this a destructive evaluation technique, the limitation to coring is that even though the results are accurate for the area from which the sample is obtained the results are unreliable for larger areas. This is a slow and laborious process making it practically impossible to collect samples for bigger structures (Lau, 1991). The suggested method for obtaining core samples by ASTM and AASHTO are ASTM C 42-99 and AASHTO T 24-02 respectively.

2.3.1.3 Chain Drag

Chain drag is a traditional technique used in bridge deck inspections, this technique helps detect distresses such as delaminations and air pockets in the bridge decks based on the acoustics of the bridge deck (AASHTO, 2011).

This general principle of the test is that when a chain is dragged along the span of a bridge deck the sound portions of the deck produce a clear ringing noise whereas the delaminated areas of the deck produce a hollow and dull sound. The inspector usually divides

the delaminated areas of the deck into grids to help him record the delaminated areas (ASTM, 1997). Alternative techniques to chain drag are Electro Mechanical Sounding and Rotary Percussion which are also based on the acoustics of the structure. ASTM D 4580-86 suggests standard procedures to perform the fore mentioned sounding tests (ASTM, 1997). A study (Chen & Scheff, 2000) aimed at understanding the acoustics of different irregularities when subjected to chain drag made some conclusions as listed below.

- Specimens with embedded rebars generated waves with a frequency between 60-80 Hz.
- Specimens with embedded cracks generated waves with a frequency between 50-55 Hz.
- Specimens with water filled cracks generated waves with a frequency between 60-80 Hz.

The results of chain drag are qualitative in nature. They are beneficial when the objective of the test is to detect the areas of the deck that has deviated from their original sound state (Chen & Scheff, 2000)

Chain drag and hammering are methods in practice by DOT's in the USA to detect distresses in advanced stages; these tests are performed under the following limitations:

- They are sensitive to the ambient conditions such as noise and weather.
- This method cannot be used on decks with overlays such as asphalt. In cases, when the decks have asphalt covering the inspectors have to remove the asphalt before sounding. In such cases the rehab work also involves costs incurred from lane closures and requires additional time.
- Chain dragging cannot be used to detect specific subsurface characteristics in a bridge deck and it is a slow and laborious procedure (Chen & Scheff, 2000)
- Acoustic methods such as chain drag, hammering or rotor percussion identify distresses only at an advanced stage.

- The projections from acoustic methods are dependent on the hearing ability of the inspector some wave frequency thus generated sometimes is beyond the hearing ability of a human ear.

2.3.2 Ground Penetrating Radar (GPR)

Ground Penetrating Radar (GPR) falls under the radar methodologies for inspection; this is one of the methods that is in use for bridge deck inspection to identify concrete deterioration and corrosion in rebars. This method is based on the dielectric properties of the bridge deck materials. This method can be used to assess the condition of bridge decks overlaid with asphalt, concrete wearing surfaces, bridge decks overlaid with Portland cement concrete and also for decks without an overlay. This method specifically detects the presence or absence of deterioration in concrete or rebar (ASTM, 2008).

GPR is currently the only available non-destructive evaluation method to assess bridge decks with an asphalt overlay without removing the overlay (Huston, Hu, Pelczarski, & Esser, 1999). This method takes a relatively lesser time to collect data and it is capable of identifying a distress in a bridge deck at an early stage before any indication of such a distress shows up on the surface, which are some important characteristics that can help save resources and improve the life of a bridge deck.

2.3.2.1 Principle and Working of GPR

All materials can be classified into either metallic or dielectric. Metallic materials are good conductors of heat and electricity, whereas dielectric materials are poor conductors. Electromagnetic waves are capable of propagating through dielectric materials and are reflected from a metallic surface (Huston, Hu, Pelczarski, & Esser, 1999). When a dielectric medium is subjected to electromagnetic waves the waves propagate through the medium until they

encounter a boundary in the medium. In this case, the boundary is change in the dielectric property of the material, when this happens part of the wave propagates and part reflects, this causes attenuation to the original wave generated from the source (Huston, Hu, Pelczarski, & Esser, 1999). The amplitude and polarity of the reflected waves from the change in dielectric properties depend upon the relative dielectric constants of changing medium (Huston, Hu, Pelczarski, & Esser, 1999).

ASTM International has published standards for Bridge Deck Evaluation using GPR in 1997, ASTM-D6087- Standard Test method for Evaluating Asphalt-Covered Concrete Bridge Decks Using Ground Penetrating Radar (GPR). The updated standards for this technique employ two different data processing methodologies. Both of the techniques employ reflection of amplitudes. One method is related to the detection of concrete deterioration and the other technique is related to the assessment of rebar corrosion.

Though a GPR test can be executed in multiple methods typical GPR test equipment consists of a source antenna to generate electromagnetic waves, a receiving antenna to measure the reflected waves, a controlling system and data storage (Vilbig & Allen, 2014). Oscillatory electromagnetic waves launched from a source antenna are directed towards the surface that needs to be examined. A receiver antenna is set up to read the reflected waves. A successful GPR setup involves several steps (Huston, Hu, Pelczarski, & Esser, 1999):

1. Electromagnetic wave Launch- the electromagnetic wave launched from the source antenna must have sufficient amplitude with proper shape and frequency so as to obtain high-resolution data. This requires an antenna that is matched to the desired frequency and wave shape, a signal source and high-fidelity cables.

2. Source antenna positioning and slewing- The source antenna should be positioned and moved in such a manner that the height from the bridge deck and the wave launch angle remain constant.

3. Receiving antenna positioning and slewing- The receiving antenna which could be the same as the source antenna must also be positioned and moved at a constant height from the deck and with a constant angle.

4. Signal processing- The data signals must be conditioned and processed properly.

5. Signal Interpretation- The output must be correlated with other forms of deck evaluation techniques such as visual inspections, infrared thermography, impact echo Testing, chain dragging and core sample collection.

2.3.2.2 Accuracy of GPR scanning

Insufficient data is available in terms of precision when it comes to detecting delaminated area in a bridge deck for this method according to ASTM (ASTM, 2008).

Also, the resolution of the output data is directly dependent upon the frequency of the electromagnetic wave generated by the source. Waves of higher frequency are capable of providing high-resolution data but they have lesser penetration. For instance, waves with a frequency of about 1 Hz have wavelengths of order 100 to 150 mm in concrete which are too big to identify the smaller subsurface features whereas, waves with frequency of about 6 Hz are capable of propagating with wavelengths on the order of 20 mm in concrete but are less capable of penetration.

Following are some studies that worked on accuracies of GPR survey. It should be noted that even though they state different accuracy results the results do not vary largely from each other.

A study on a sample of ten bridge decks at New York, Virginia, and Vermont using the GPR attenuation technique gave an output of error +/- 11.2% in terms of deck area (ASTM, 2008).

A Study by (Huston, Hu, Pelczarski, & Esser, 1999) achieved an accuracy of +/- 3mm for depth of distresses over 40 readings for frequencies of 2.6 GHz i.e. about 6-7% of surface course thickness, which the authors believe is sufficient.

A report by Infrasense states that some studies show the accuracy of quantity estimation to be about 3.5 %, an accuracy of depth of underlying features are within 10 % of the results obtained from analyzing cores (INFRASENSE, Inc., 2014).

2.3.2.3 GPR Data Acquisition

The data acquisition techniques can be classified into two major categories based on the position of the antenna at the time data acquisition. When the antenna used is in contact with the ground at the time of data collection the technique is referred to as ground-coupled GPR. When the antenna used is operated from a height it is referred to as air-coupled GPR. The selection of equipment is based on the level of accuracy required and the time factor involved.

Data acquisition from height allows the air-coupled antennas to be mobile thereby making the data acquisition procedure faster. When it comes to collecting data from a series of bridges or long bridge using a faster technique like the air-coupled antenna makes lesser interruption to traffic and saves a lot of time. On the other hand, ground-coupled GPR is capable of producing higher resolution data. This is mainly because the ground-coupled antennas can achieve more penetration allowing the usage of waves of higher frequency. Since the waves are narrower the data obtained is much denser i.e. more scans per unit length along the data

collection path. Higher resolution data allows Ground-coupled GPR to observe low angle cracking and other barely visible defects (Gucunski, et al., 2011).

2.3.2.4 Processing and Analysis of GPR Data

There are two accepted methodologies for processing GPR data both these methods are based on the reflected wave amplitudes. The two methods are bottom deck attenuation method and top reinforcement reflection attenuation method. In the bottom deck reflection attenuation technique, the deterioration estimation is projected using relative reflection amplitudes from the bridge deck bottom relative to the bridge deck surface. In the top reinforcing reflection attenuation technique, the relative reflection amplitudes from the top layer of reinforcement are used to understand the deterioration (ASTM, 2008).

2.3.2.4.1 Bottom Deck Reflection Attenuation Technique

When the deterioration at top of steel reinforcement is measured using bottom deck reflection attenuation technique the following steps are followed (ASTM, 2008).

- The strength of the signal applied at the deck surface is measured and recorded as V_t and then the maximum strength of the echo from the bottom of the deck is recorded as V_{bs}.
- If V_{bs} is less than 0.0264 V_t after repeating the longitudinal inspection pass it means the data is not reliable for measuring the distresses in the bridge in such a case data must be processed using an alternative technique.
- If V_{bs} is greater than or equal to 0.0264 V_t then the amplitude of the deck bottom echo V_b is measured for each weave form (0.0264 is a value obtained using research data).
- The concrete is considered delaminated if V_b is less than or equal to 0.385 V_{bs}.

The percentage of delaminated area and the estimated quantity of deck delaminated at the top of steel for each GPR inspection pass can be calculated using the following equations (ASTM, 2008).

$$X_{tn} = [W_{dt} / (W_{dt}+W_{st})].100 \quad (3)$$

Where,

X_{tn} = percent delaminated in inspection pass, n, at top steel

n = GPR inspection in a GPR inspection pass identification number

W_{dt} = Concrete delaminated in a GPR inspection pass number

W_{st} = Sound concrete at top steel, m

$$Q_t = (X_{tn}). (L_n). (d_t) \quad (4)$$

Where,

Q_t = Area of deck delaminated at top of steel in Square meters

L_n = Length of GPR inspection pass, n, in meters

d_t = transverse distance between GPR inspection passes, in meters

$$Q_{Tt} = \sum Q_t \quad (5)$$

Where,

Q_{Tt} = Total area of deck delamination at top steel for all GPR inspection pass in Square meters.

2.3.2.4.2 Top-Reinforcement Reflection Attenuation Technique

Top reinforcement attenuation technique is only appropriate for structures that have main reinforcement placed uniformly in the direction transverse to the direction of traffic. This method is not appropriate when the main reinforcement is placed along the direction of travel mainly because of the variation in steel density along the direction of travel. The method is also not

suitable for decks having top reinforcement placed at more than 8 in. spacing. In such cases mentioned above the inspector can use alternative methods such as bottom deck attenuation technique or ground coupled antenna (ASTM, 2008). The main reinforcement in this type of deck should be transverse to the traffic. It spans across the stringers. Slab on stringer type structures, arch slabs, one-way slabs are some examples of structures with reinforcement along the direction of traffic (Tonias, 1995).

The first step in deterioration measurement using top reinforcement reflection attenuation technique is to extract the amplitude of the reflected waves from the top layer of reinforcement. The data processing for air-coupled antenna depends on factors such as frequency of the antenna used, the type of bridge and the thickness of asphalt.

According to suggested methods by ASTM International, the air-coupled GPR antennas are used on asphalt-overlaid bridge decks are of typically either 1 GHz or 2 GHZ frequency antennas. When a 1 GHz antenna is used on asphalt-overlaid bridge decks with rebar cover greater than two inches the data processing involves subtraction of metal plate reflection from each scan. When bridge decks with asphalt overlay of less than two inches rebar cover are inspected using 1 GHz antennas the data collection needs to be done using two antennas aligned with the longitudinal direction and radiating perpendicular polarizations. This is due to the possible interference between the asphalt-concrete interface reflection and the rebar reflections. The data processing involves the following when air-coupled antennas are used.

- When inspecting asphalt-overlaid bridge decks with rebar cover greater than 2 in. and concrete surface decks the first step is to subtract metal plate reflection from each scan.
- When inspecting asphalt-overlaid decks with rebar cover less than 2 in. an additional step to remove clutter is done before subtracting metal plate reflections. Clutter is the

unwanted echo that occurs in data collected due to the close proximity of the rebars.

- In such cases where the top reinforcement is not near 45 degrees to the direction of traffic, the reflection of top layer reinforcement is isolated from bottom deck reflections.
- The next step is to record the highest amplitude of top reinforcement reflections from the data put through the initial step.
- The reflection amplitudes are then converted to decibels using eq. (6).

$A_{dB} = 20\log_{10}(A)$ (6)

A_{dB} = Reflection amplitude in decibels

A = Reinforcing reflection amplitude in data units

The lower the reflection amplitude the higher the possibility of deterioration. The areas of the deck having reflection amplitudes 6 to 8 dB less than the maximum reflection amplitudes typically correspond to the delaminated areas. This inference is made from results indicated by core data and results from other inspection techniques for deterioration estimation (ASTM, 2008).

2.3.2.4.3 Ground Coupled Antenna Data Processing and Analysis

Processing and analyzing a high-resolution GPR ground coupled data to create a deck deterioration map involves three major steps (Gucunski, et al., 2013).

- The first step is Time zero correction of surface signal. In this step, the reflected wave from the backside of concrete layer that shifts to a later time when an antenna is coupled to the medium is corrected to time zero. This occurrence of a shift in time is known as ‘Radiation delay’ this phenomenon is more dominant in surfaces with high moisture content. Time zero correction is a very crucial step for accurate data.
- The second step is rebar reflection picking which are verified in the third step.

- The third step is interactive interpretation in which the reflected data is reviewed and edited. The output of this process is a table with rebar position and amplitude of reflection.
- An optional step of migrating hyperbolic waves reflected from the rebar can be done between step one and step two.
- The reflection amplitudes are then converted to decibels using Eq. (6).

The reflection amplitude data in decibels is analyzed to estimate the deteriorated areas using the same procedure used in top reinforcement attenuation technique.

The next procedure is to present the data obtained from the output after data processing and analysis. This process is done by presenting the attenuated signal at rebar level in the form of a contour map thus representing the relative deterioration on the deck in form of a contour map (Gucunski, Romero, Kruschwitz, Feldmann, & Parvardeh, 2011). Color-coded contour plots are generated from the amplitude of reflection at rebar level as the gradient in the plot. The color-coded contour maps in some cases can also be made for rebar depth variations when data of high accuracy is available. These maps usually use hotter colors such as reds and yellows to represent higher levels of a deterioration and the cooler colors such as greens and blues to represent areas that are in good condition (Gucunski, et al., 2011). The percentage of the delaminated area and the estimated quantity of delamination can be estimated using equations (3), (4) and (5).

The procedures for obtaining the reflection amplitudes for the three procedures in this section are explained using flow charts using figure 1, figure 2 and figure 3.

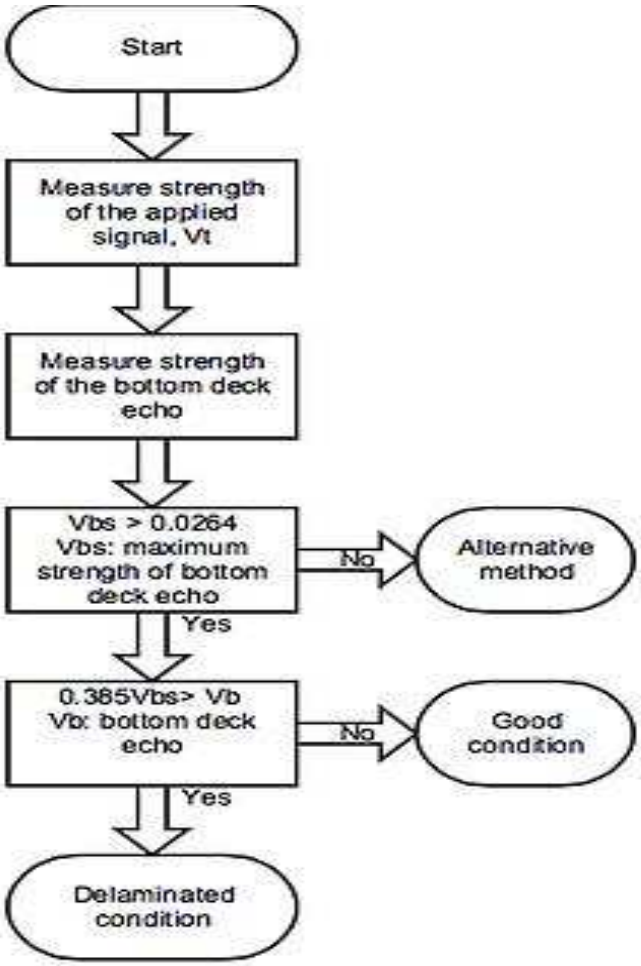

Figure 1: Finding delaminated areas using bottom deck attenuation technique (ASTM, 2008)

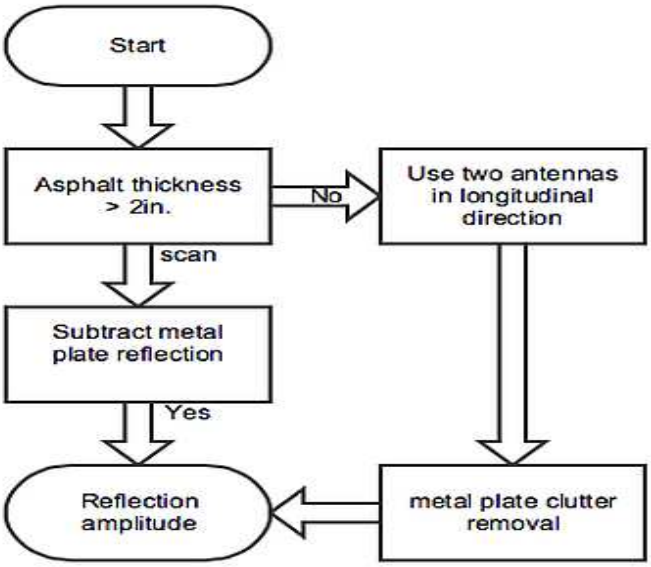

Figure 2: Data processing to obtain reflection amplitudes using top reinforcement attenuation technique with 1 GHz air coupled antenna (ASTM, 2008)

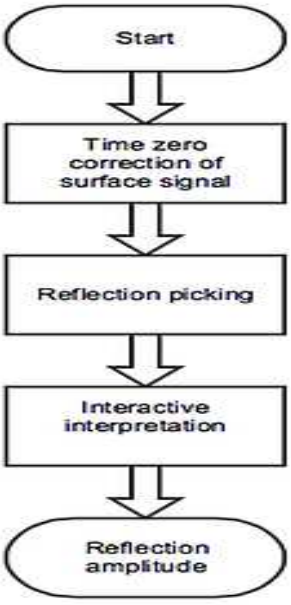

Figure 3: Data processing to obtain reflection amplitudes when using ground coupled antenna (ASTM, 2008)

2.3.2.5 Applications of GPR

GPR is currently the only available NDE to analyze asphalt-covered decks. It allows the inspector to analyze the top flange of a box area, which is otherwise inaccessible (AASHTO, 2011).GPR is capable of detecting changing mediums this allows the bridge inspector to detect the underlying features such as rebar depth, the bottom layer of asphalt cover. The loss in concrete cover can be determined from the rebar depth. A loss in concrete cover reduces the protection to underlying reinforcement making the deck more vulnerable to corrosion. GPR scans allow the inspector to find areas with loss in cover and take necessary action (D.Ciampa, 2009).

Scaling in decks can lead to problems such as spalling in advanced stages. When Scaling is present under the surface of decks in areas such as the concrete pore structure it cannot be detected through visual inspections. Such an occurrence can easily be detected using GPR because areas with scaling have high dielectric properties (INFRASENSE, Inc., 2014).

GPR technology can also be used for quality control purposes to inspect newly built roads. Inspectors can find the thickness of roadways, subgrade thickness, asphalt cover, concrete cover, etc., when roads are constructed using GPR technology the current practice to make such inspections is to obtain core samples from discrete locations. Ensuring proper quality makes the structure more durable, which is an important feature for structures such as bridges (Vilbig & Allen, 2014). The as-built data of a structure such as bridge decks can be obtained using GPR technology (Vilbig & Allen, 2014).

The sensitive nature of GPR to corrosion help in mapping the severity of probable deterioration (Gucunski, et al., 2013). The Current research in this field is focused upon three main categories; corrosion of reinforcement, electro-magnetic properties of the pavement and

voids or delaminations. All these categories attempt to identify the level of deterioration in bridge decks and typically one of these problems will lead to the other (Vilbig & Allen, 2014).

The dielectric properties of materials are functions of density, moisture content and chloride content in a material (INFRASENSE, Inc., 2014). This opens up to a possibility of understanding more about material properties through the GPR data.

2.3.2.6 Limitations of GPR

GPR is not capable of directly imaging delaminations unless the delaminations are filled with water or impregnated with epoxies (Gucunski, et al., 2013). Areas that represent signal attenuation include joints and curbs. The areas projected by GPR are not necessarily deteriorated because the attenuation could be due to corrosion or related damages such as infiltration and ponding of chlorides into these regions (Gucunski, et al., 2011).

GPR results are easily influenced by frozen moisture in the decks and the infiltration of deicing salts used during snow periods this due to the change in dielectric properties of the deck (Gucunski, et al., 2013).

GPR test may not be suitable in the cases where delaminations are localized over the diameter of the reinforcement (ASTM, 2008). GPR is not capable of producing definitive results on rebar corrosion or loss in rebar section (Gucunski, et al., 2011).

This method is also not suitable for bridges with cathodic protection or for bridges in which conductive aggregates have been used (ASTM, 2008). Hence, when using GPR is a long-term plan the owner of the bridges has to consider alternatives to cathodic protection.

2.3.3 Infrared Thermography (IR)

Infrared (IR) thermography method is carried out using infrared cameras that are capable of recording infrared radiations from the target body. Infrared waves are waves of wavelength in the range between 0.7 and 1.4μm. The cameras capture the infrared radiation and process them into electrical signals, which can be further processed into subsurface temperature maps. This is possible because the electromagnetic radiation wavelengths from an object are related to temperature variations in infrared waves. It has been a common practice since the 1980's to use infrared cameras to detect delaminations, cracks, and deterioration in concrete (Zachar & Naik, 1991).

Since the first research in 1973 on infrared thermography by ODOT (Ontario Department of Transportation), numerous publications have targeted the accuracy of IR one such paper Love, 1986 claims that Infrared thermography has an accuracy of about 97% (Zachar & Naik, 1991).

2.3.3.1 Principle and Working of IR

The distribution and flow of heat in a material are functions of three specific material properties, which are thermal conductivity, density, and the specific heat capacity. Infrared cameras capture the thermal radiations that vary with the thermal properties of materials and present the varying temperatures in the radiation (Gucunski, et al., 2013).

Distresses such as delaminated areas and cracks are usually filled with air or moisture that have different thermal conductivity in comparison to sound concrete. Hence, at the time of heating or cooling of a deck from the sun in the mornings or evenings, the air or moisture filled parts of concrete heat up and cool down faster. This process of heating or cooling in sound

concrete results in temperature differences of 1^0 to 3^0 C with the surrounding areas (INFRASENSE, Inc., 2014).

The temperature variations also depend on elements filling up the delaminated areas and cracks. For instance an air crack of 0.05 in. width can reach a temperature difference of +/- 4^0 C to the temperature of sound concrete. When a similar crack is filled in water the temperature difference could be about 0.2^0 C, which is hard to detect (Zachar & Naik, 1991).

2.3.3.2 Analysis of Infrared Images

The infrared images can be used to differentiate delaminated areas from deboned areas in case of decks covered in the overlay. This is possible due to the difference in the nature of thermal signatures. The debonded regions generally have uniform temperatures and appear as smaller circular regions where as delaminated areas are typically larger non-circular and have non-uniform temperatures.

2.3.3.3 Limitations of IR

Cloudy conditions are capable of reflecting the infrared emissions and slowing down the heat exchange process (Zachar & Naik, 1991). As the method also requires the deck to be in the state of heating or cooling down this method cannot be used on decks that lack proper exposure to sunlight.

Windy conditions are capable of accelerating surface temperatures, which could negate the temperature differences caused by the subsurface irregularities. Moisture can increase the dissipation of heat there by negating the temperature differences occurring in the deck (Zachar & Naik, 1991).

The results of IR do not give the depth of anomalies and IR is not capable of detecting deep anomalies. IR results are also sensitive to boundary conditions due to the active heat transfer to or from adjacent lying materials at edges (Gucunski, et al., 2011)

3. DATA COLLECTION

3.1 Introduction

As mentioned earlier in the motivation of this research, The Colorado Department of Transportation (CDOT) pays contractors for a unit area of deck removal based on the class of the deck removal.

Another factor to consider during evaluation of bridge decks is that CDOT considers replacing the entire deck in a bridge for condition states worse than 5 on National Bridge Inventory (NBI) rating. Bridge deck deterioration is said to be 5 or beyond on NBI rating when the combined area of repaired areas and/or spalls/delaminations is more than 25% of the total bridge deck area. Refer appendix B for more detail on guidelines to NBI ratings of concrete bridge decks followed by CDOT.

It is important to have an accurate estimation of the removal quantities categorized by the classes, as the cost of removal for each of these classes is different. The major issue has been that the estimated removal in the deck when sounded is found to be deviating from the damage detected when these areas are chipped. The inspectors cannot estimate the removal classes with sounding the deck. There is a need to improve the methods to estimate damaged area. In some cases, the inspectors discover that NBI rating is 5 or more after the chipping process. Hence, the inspectors are evaluating alternative methods to sounding and chipping for bridge deck inspections.

3.2 Deck Evaluation Methods Used

The decks were evaluated by using two different procedures. The first was carried out by Infrasense, Inc., a firm that has evaluated over 1200 bridge decks in the USA using a similar

procedure. Infrasense uses a combination of infrared thermography, GPR scans and visual inspections to predict deteriorated areas by their classes. This is an alternative method to sounding and chipping procedure that is being considered for bridge deck evaluation. The second procedure of sounding and chipping was carried out by Tsiovarras Simmons Holderness (TSH), a Colorado-based engineering consulting firm. TSH personnel performed sounding over the concrete deck after removing the asphalt overlay using chain drag, rotary percussion, and hammering. Each procedure is described in detail in the following sections.

3.2.1 GPR and IR Evaluation of Bridge Deck

Distinct evaluation methods are used by Infrasense to detect areas of class-1, class-2 and class-3 damages. Data collection and analysis techniques for each class of deck removal are explained in detail in this section.

3.2.1.1 Estimation of Class-1 Areas

The class-1 regions are estimated using infrared thermography as suggested by ASTM D4788–03, which is appropriate for use on bridge decks overlaid with Portland cement concrete mixtures. The inspection is carried out using a setup mounted on a survey vehicle, which includes the following:

- A high-accuracy EDM (Electronic Distance Measurement) encoder to record the distance and control the data collection process. This equipment is attached to the inspection vehicle's wheel.
- An infrared camera (FLIR A40M) mounted on an elevated platform on the inspection vehicle.
- A 45-degree wide lens to capture the entire width of the lane.

- A high-resolution video camera (VIRB camera) integrated with GPS.
- Software customized for infrared bridge deck images. The software creates infrared video strips from a sequence of infrared images, producing infrared plan area view of bridge deck surface capable of producing maps compatible with AutoCAD.

The setup used is capable of collecting data from a width of 12 to 15 ft. on a typical two-lane deck with a shoulder on each side of the deck while it is traveling at speeds of about 50 mph. To obtain maximum temperature differentials caused by the delaminations and debonding in the deck when using the infrared camera the data collection process is carried out between 10 a.m. and 5 p.m. The weather conditions are also taken into consideration at the time of data collection. Which include decent amounts of solar radiation on the deck surface and a temperature difference of 10^0C between day and night times.

The output of this procedure is a series of infrared and visual images along the travel lanes on the deck. This data is processed using software programs into maps that are compatible with AutoCAD.

Data processing for class-1 regions:

The center foot of each pass is laid adjacent to the following pass from edge to edge to obtain a thermal image of the entire bridge deck. The infrared data is compared to video data to pick areas with surface features that could affect the infrared images such as oil stains, discoloration, rust, sand deposits etc. These surface anomalies are unrelated to subsurface conditions in the deck. For decks with overlays, the subsurface condition of interest is overlay debonding which are usually brighter spots in the infrared images.

The infrared images show areas of damage as white blotchy spots. These white blotchy spots are hot spots occurring due to the thermal barrier. Which can be related to delaminations in

the deck or debonding of overlay in the case of decks with overlay. The blotchy areas over the deboned areas are characterized to be brighter than areas that are delaminated. The blotchy white regions are outlined using computer software and presented on a deck plan as areas of class-1 damage.

3.2.1.2 Estimation of Class-2 Area

The GPR analysis method adopted by Infrasese and other firms detects deterioration at or below the top rebar level. Hence, the deteriorated areas indicated by GPR are classified as class-2 areas. The procedure suggested for GPR inspection of bridge decks is ASTM D6086-08. The equipment and procedure used by Infrasense exceed the suggested standards in ASTM D6086-08. The setup used for GPR inspections is mounted on a survey vehicle with the help of a mobile mounting system. The setup includes the following equipment.

- A high-accuracy EDM is attached to the wheel of survey vehicle to measure the distance continuously and to control the data acquisition process
- A GPR data acquisition system approved by FCS (federal communication system) SIR-20 is operated from inside the vehicle to acquire data and control the acquisition process
- Horn antennas of 1.0 GHz frequency manufactured by Geophysical Survey Systems, Inc. (GSSI) are used to generate GPR waves and record the reflected waves. These antennas are mounted using a rectangular mounting bar that can adjust the lateral position of each antenna. This enables the GPR survey to cover the entire width of the deck without needing to straddle on the lanes

- winDECAR, an advanced GPR data processing software for analysis and interpretation of bridge deck data is used to process the GPR data. The outputs of this software are CADD compatible and meet the specification of ASTM D6086-08

This setup is used to collect data from inspection vehicles when traveling at speeds up to 60 mph. The survey vehicle collects the data from a series of longitudinal passes starting from a distance of about 200 feet before the point from which the data is required. The setup is capable of collecting data at a resolution of 4 scans per linear foot. The location of each pass is approximately determined using visual reference points and lane markers. The data collected along with the distance at which the data is collected is recorded, digitized and stored in a hard disk.

When reflected GPR waves from the deck are measured, the reflected wave properties such as time and amplitude can be used to measure the underlying subsurface features and wave attenuation. Wave attenuation can be related to dielectric properties of the deck. Dielectric constant is a function of density, chlorides and moisture content. Hence areas with corrosive environments, high chloride content and delaminations will reflect attenuated waves. Reflected waves below a statistically determined threshold are estimated to be areas with distresses.

GPR is capable of detecting delaminations and rebar corrosion at or below top rebar level but the actual depth of these distresses cannot be projected. Hence, GPR results are used to estimate the quantities for Class-2 deterioration.

3.2.1.2.1 Class-2 Area Data Processing

The class-2 data processing executed by Infrasence is explained using the data deck condition reports produced by Infrasence. The analysis procedure is carried out using software called winDECAR. The procedure starts with identifying the ends of the bridge deck and

checking the distance. The distance is identified using the data measured and recorded by the EDM against reference points on deck such as known distances and deck features. Following this the subsurface features of the deck such as deck thickness, rebar cover, and thickness of overlay, which act as dielectric discontinuities are identified. Further analysis is carried out to find out the dielectric constant of the concrete and the wave attenuation. The results of this process and the identified underlying features are setup for all the passes on the deck

The potential areas of deterioration recognized from GPR data analysis are mapped as contour plots. The areas of potential deterioration are identified using a threshold value of wave energy determined from statistical analysis of the obtained data categorizing areas with weakened signals as deteriorated areas. These areas are associated with chloride and moisture infiltration, rebar corrosion or delaminations at rebar level.

Since each deck has different material properties based on the material properties and construction methods used, the resulting wave properties are different for each deck. Hence, the threshold values are calculated separately for each deck.

The severity of deterioration in concrete is represented numerically on a scale of 0-1.0, based on the deviation of the wave energy from the threshold value. The severity is also represented in the contour map on a colors scale from blue to magenta, using blue for less severe regions and magenta for more severe regions.

3.2.1.3 Importance of Visual Records

Both GPR and Infrared techniques are sensitive to changes in material composition. Hence, the results from both techniques are affected by surface patching. Infrared is also sensitive to surface elements such as oil, water or paint on the deck. Hence, the recorded visuals

are used to find such areas. Patched areas that overlap with IR or GPR are included in the estimated repair quantities.

3.2.1.4 Estimation of Class-3 Areas

Estimation of class-3 areas plotted in reports produced by Infrasense is based on visual surveys of the underside of the bridge deck conducted by TSH personnel. The objective of this survey is to find conditions indicating full deck deterioration such as moisture infiltration, spalling, cracking, rust staining, efflorescence and other signs of distress. The information from the underside survey serves as the basis for quantifying class-3 deterioration in decks. This data is compared with the estimations made from GPR and IR to account for overlapping regions at the time of quantity calculation.

3.2.2 Sounding by TSH

The current method used for determining deck removal areas in Colorado is sounding and subsequent removal of delaminated regions by chipping. The sounding on the deck is carried out along the guidelines of ASTM 4580-86 after removing the overlay and cleaning up the surface of the deck from debris. The inspection is carried out using chains, hammers, and rotary percussion. The decision on which equipment to use at each location is made by the inspector carrying out the inspections. This process of detecting delaminations does not involve detecting the class of removal.

The class of removal, which is the basis for payment to the contractor is discovered at the time of deck removal based on the depth of removal at the locations identified by sounding. The estimation of class-3 areas is additionally made from visual inspections i.e. when the inspector

finds distresses at the bottom of deck indicating full depth deterioration in concrete, those areas are identified as Class 3.

4. ASSESSMENT OF AVAILABLE DATA AND INFERENCES

4.1 Data Used

The data used for this study is from four decks G-26-T, G-26-U, G-26-S and G-26-B. The data includes the estimations for different removal classes prepared from GPR, IR, visual inspections, sounding, coring and as-built data. The data from the GPR scanning includes subsurface features such as rebar depth, concrete cover and ac-overlay thickness estimations along with the severity of concrete deterioration. The concrete cover and ac-overlay thickness in the GPR report are represented in contour maps with unique colors for each depth. These decks were rebuilt the spring of 2015 after sounding and chipping. The data related to sounding and chipping is available in the form of as-built data.

4.2 Preparation of Data for Assessment

This section explains the procedure for preparation of overlays used for observation. The estimations made by GPR, IR and visual inspections along with the patching work are overlaid on plans of the bridge deck. These overlays are prepared using the images provided in the deck inspection reports prepared by Infrasense. The images are overlaid on the deck plans and the estimated areas are picked using mouse cursor to calculate the areas. The areas estimated by each method are plotted on the deck plans with unique colors. The quantitative output of this procedure is sorted into tables for further observation.

4.2.1 Step-1: As-built Data Overlay Preparation

The geo-spatial co-ordinates of as-built data are recorded manually using structural features such as abutments, piers, and railings as reference points. These Geo-spatial coordinates

are used to prepare the overlays of the as-built data into the deck plans prepared in AutoCAD. The as-built data in AutoCAD is plotted with unique colors for each removal depth. Geo-spatial coordinates can alternatively be collected using GPS equipment. The advantage of using GPS equipment is that the spatial coordinates can be recorded quickly and stored digitally in the GPS equipment. The stored co-ordinates can be plugged into AutoCAD directly from the GPS equipment.

The plans of each deck are prepared using AutoCAD. The sketches and notes of geospatial co-ordinates prepared at the time of removal are used to plot the removal areas on the deck plan in AutoCAD. Each class of removal is given a unique color. Figure 4 is an example explaining the preparation of as-built data overlay on the plan of G-26-B using AutoCAD.

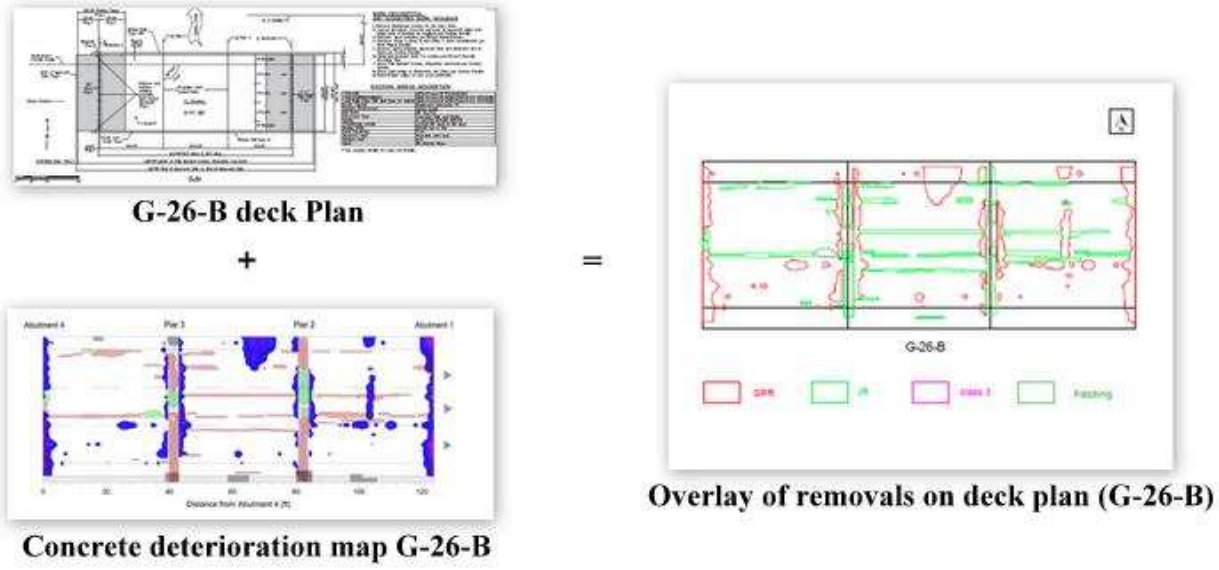

Figure 4: as-built overlay preparation

4.2.2 Step-2: GPR and IR Data Overlay Preparation

The condition reports produced by Infrasense consisting of NDE reports are used to obtain maps of concrete deterioration. The NDE estimations are overlaid on the deck plan to

scale in AutoCAD. These areas were traced to the deck plan using mouse cursor. Such an overlay typically includes estimations for class-1, class-2, and class-3 removals along with the existing patching work. Unique colors are provided for each of the estimations and patching. Figure 5 is an example of the procedure used for preparing a map of concrete deterioration in deck G-26-B using NDE reports.

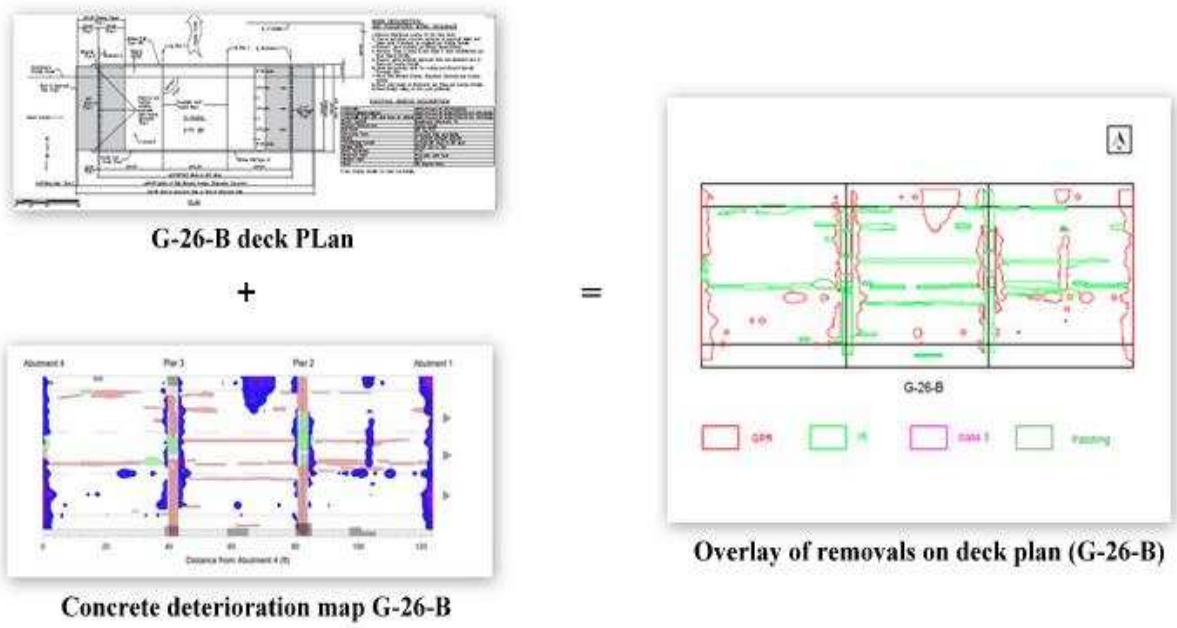

Figure 5: Removals estimation map preparation from NDE data

4.2.3 Step-3: Concrete and Asphalt Overlay Data Preparation

The condition report from Infrasense is used to obtain the images of asphalt overlay and concrete cover estimations on the entire deck area. These images are overlaid on the output file obtained from step-2 to separate layers in AutoCAD. The transparency of the layers with these images is increased to 75%. The reduced transparency allows the observer to visually compare the concrete and asphalt cover data, the estimated removal classes and the as-built data. Figure 6

shows an example of the procedure followed to build overlay of asphalt cover for deck G-26-B in AutoCAD. Each overlay is plotted in a different layer in AutoCAD this helps us control the overlays that we intend to compare.

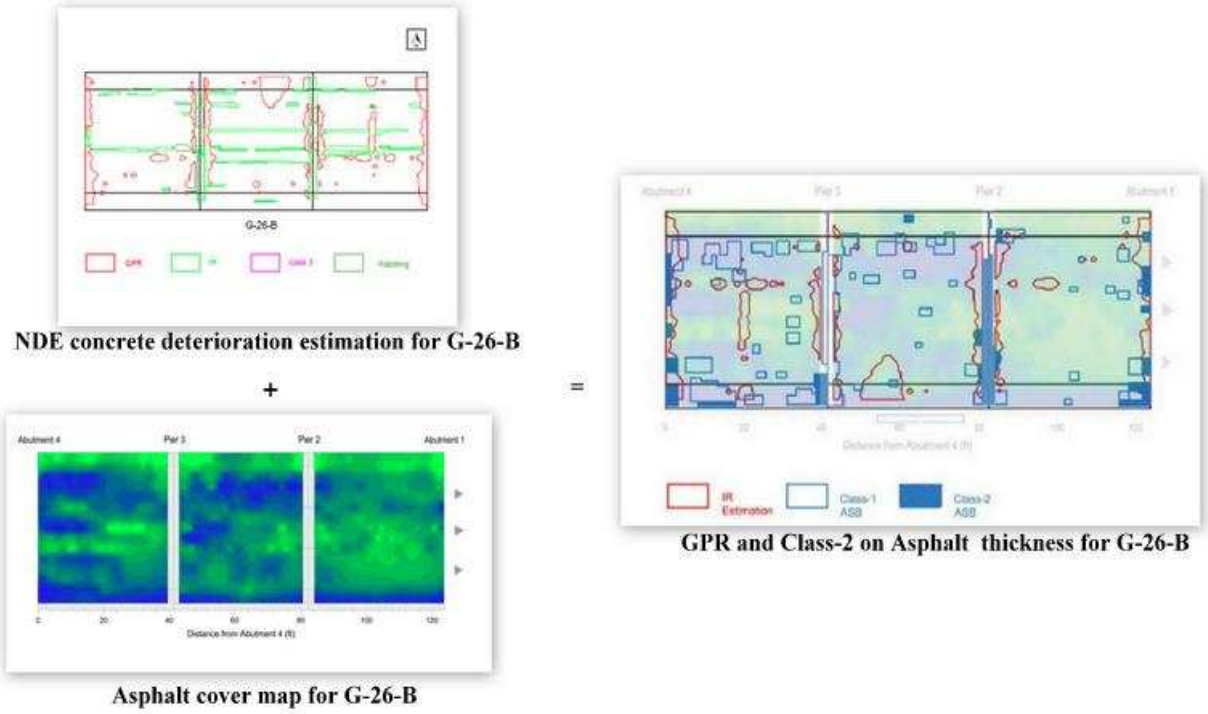

Figure 6: Preparation of asphalt cover overlay with class-2 estimations and removals

4.2.4 Step-4: Sorting Data for Observation

There are two sets of data available for this study after preparing all of the overlays in AutoCAD. The first set of data is the Infrasense reports and as-built data. The second set of data is the data that can be extracted from overlays of the first set of data in AutoCAD. The two sets of data are combined and sorted into 5 tables for quantitative observation. The rest of this section explains how the data is organized into each of these tables and the purpose of sorting specific data into each tables.

Table 5 consists of basic condition data of each bridge deck which includes the year built, NBI ratings, deck element condition states, total deck areas, average concrete cover and asphalt

cover. Table 5 meant to provide insight on the state of each bridge deck examined in this study. The average concrete cover and asphalt cover data is obtained from Infrasense reports. The calculation of the thickness of covers is explained in section 3.2.1.

Table 5: Bridge decks inspected and condition data

Bridge	**Year built**	**NBI rating**	**Deck element state condition**	**Total deck area**	**Average concrete cover**	**Average asphalt cover**
Units	N/A	N/A	N/A	sq. ft.	in.	in.
G-26-U	1970	5	1	8736	3.4	2.9
G-26-T	1970	7	1	5937.6	3.7	3.4
G-26-S	1965	6	1	7907.80	3.2	2.1
G-26-B	1964	6	2	5690.2	3.8	3.9

Table 6 consists of the summary of scanning results from condition reports produced by Inrasense. The data includes the estimations of each class of removal, patched areas and the areas not accessible for GPR. The areas not accessible to GPR are calculated using AutoCAD from the concrete deterioration maps in condition reports. The purpose of calculating the areas not accessible to GPR is to help us understand the impact of accessibility limitation of GPR and to further examine the data we have for such areas.

Table 6: Summary of survey results from using GPR and IR thermography

Bridge	**Estimated areas through NDT evaluation**			**Patched areas**	**Areas not accessible to GPR**	
	Class-1	**Class-2**	**Class-3**		**Total**	**Class 2 ASB**
Unit	sq. ft.	sq. ft.	sq. ft.	sq. ft.	sq. ft.	sq. ft.
G-26-U	472	1345	192	0	169	13
G-26-T	558	517	65	0	116	92
G-26-S	293	2594	127	55	615	296
G-26-B	398	609	131	80	159	109

Table 7 is a summary of as-built data after sounding and chipping the entire deck area. The table consists of total removals of each class and the data areas that are correlating with the estimations made using NDE techniques. The correlating areas are calculated as the common area of estimations made using AutoCAD. These correlating areas help us compare the two evaluation techniques.

Table 7: Summary of deck as-built data

Bridge	**As-built data from sounding and chipping**		**As-built area correlating with NDT findings**	
	Class-1	**Class-2**	**Class-1**	**Class-2**
Units	sq. ft.	sq. ft.	sq. ft.	sq. ft.
G-26-U	662	165	58	4
G-26-T	399	254	16	15
G-26-S	387	1242	9	466
G-26-B	605	263	15	151

Table 8 and Table 9 consist of data comparisons between NDE estimates and as-built data for each class of removal. **Error! Reference source not found.** consists of the comparisons as a percentage of total deck area and the accuracy of IR results for each of these decks.

Table 9 is a summary of the percentage of as-built data correlating with GPR, the accuracy of GPR and the data regarding the class-2 removals in areas not accessible to GPR. The limitations of both GPR and sounding are taken into consideration when calculating the accuracy of GPR from the available data.

The areas inaccessible to GPR usually include the areas along the expansion joints and these areas are estimated to be class-1 when infrared cameras suggest deterioration. This data regarding GPR inaccessible areas is calculated for quantitative observation as the overlays indicated that such areas were actually repaired as class-2. The data includes class-2 removals as a percentage of total inaccessible areas and the class-2 removals in inaccessible areas as a percentage of total class-2 areas. The purpose of calculating these percentages is to observe the

comparison between class-2 deterioration and areas that are inaccessible to GPR. The accuracy of GPR is calculated only for areas that GPR can access.

4.2.4.1 Inaccuracy Calculation of NDE Methods

The inaccuracy calculation in this study assumes that 100% of the area indicated by GPR and IR scans as deteriorated are deteriorated. This assumption is made considering the fact that we have insufficient data regarding the areas that do not correlate with sounding and chipping. Sounding and chipping cannot find corrosive environments or areas in early stages of deterioration. This assumption allows a benefit of doubt to the NDE methods and keeps our focus on regions that required repair that have not been discovered by either GPR or IR.

The calculation of inaccuracy of the NDE methods is explained using Venn diagrams for each deck. The circle to the left hand side in each diagram represents the estimate made by the NDE method and the circle to the right side represents the respective class of removal from the as-built data. The common area in the Venn diagram is the correlating area between the NDE findings and the as built data. The total area of the Venn diagram represents the total deterioration of the respective class of removal. The inaccuracy is calculated as the class of removal not correlating as percentage of the total area of the respective class i.e. total area of the Venn diagram.

$$Inaccuracy\ of\ NDE = \frac{B}{(A+B-C)} * 100 \quad (7)$$

Area of a specific removal class estimated by NDE = A

Removal area of the removal class from as-built plans = B

Area where NDE and as built data match for a given removal class = C

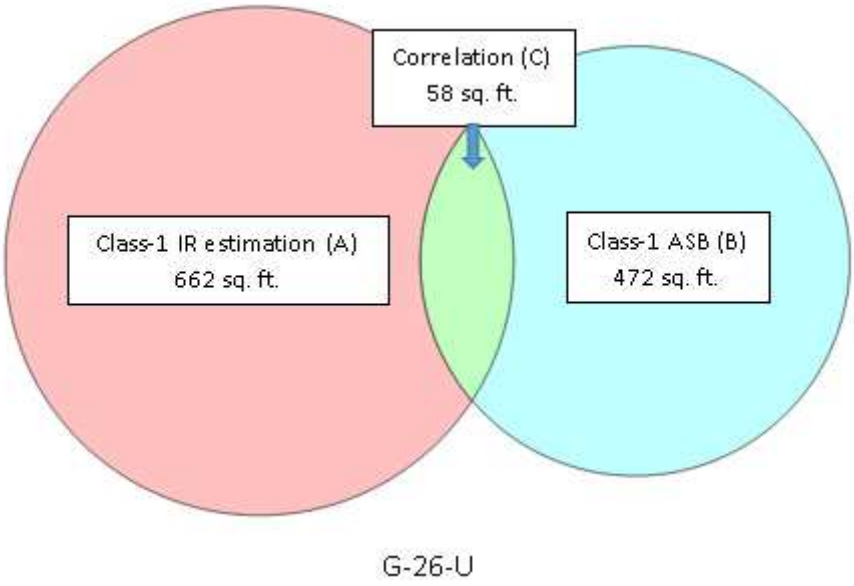

Figure 7: Comparison of G-26-U class-1 data

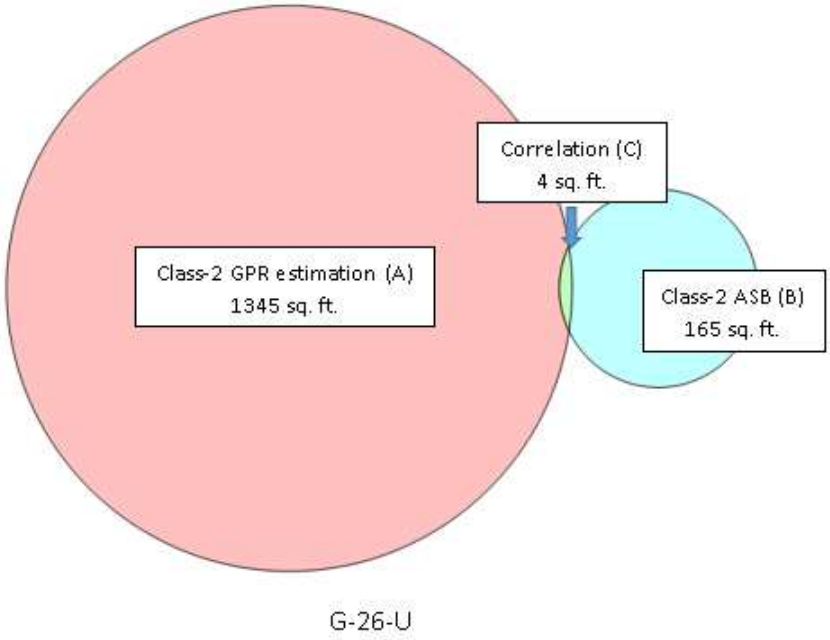

Figure 8: Comparison of G-26-U class-2 data

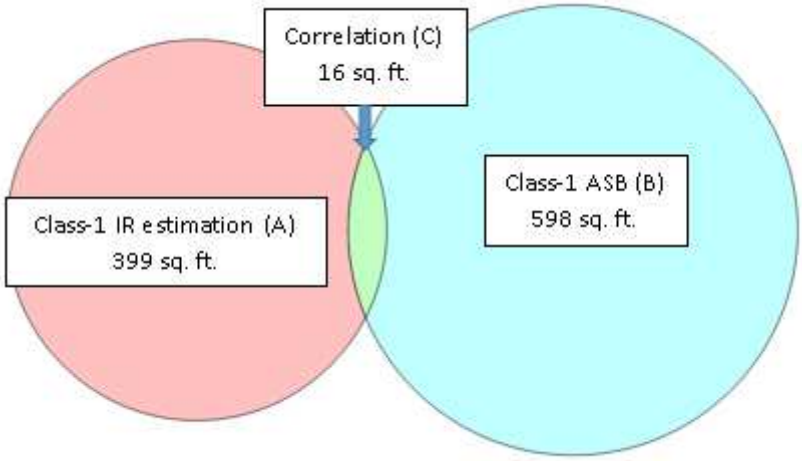

G-26-T

Figure 9: Comparison of G-26-T class-1 data

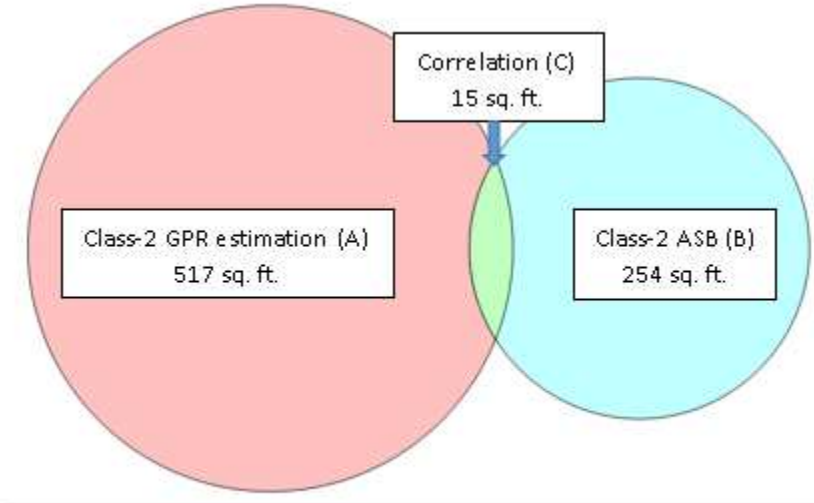

G-26-T

Figure 10: Comparison of G-26-T class-2 data

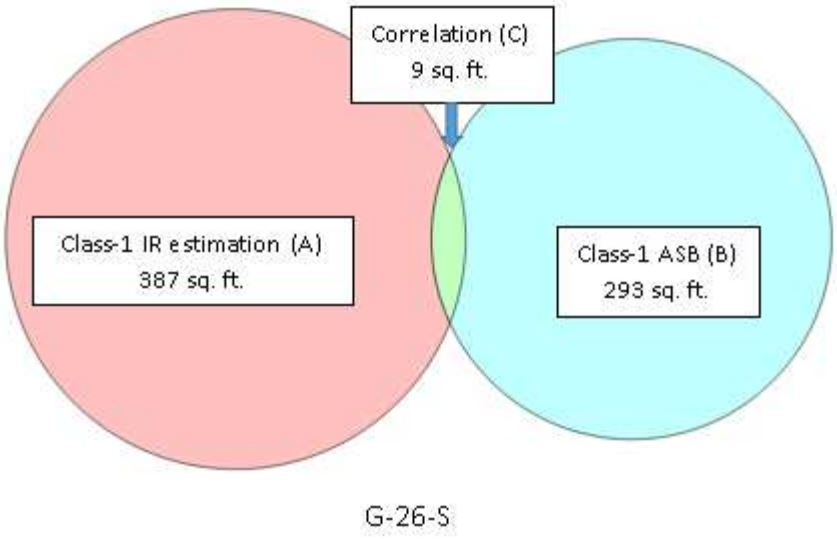

Figure 11: Comparison of G-26-S class-1 data

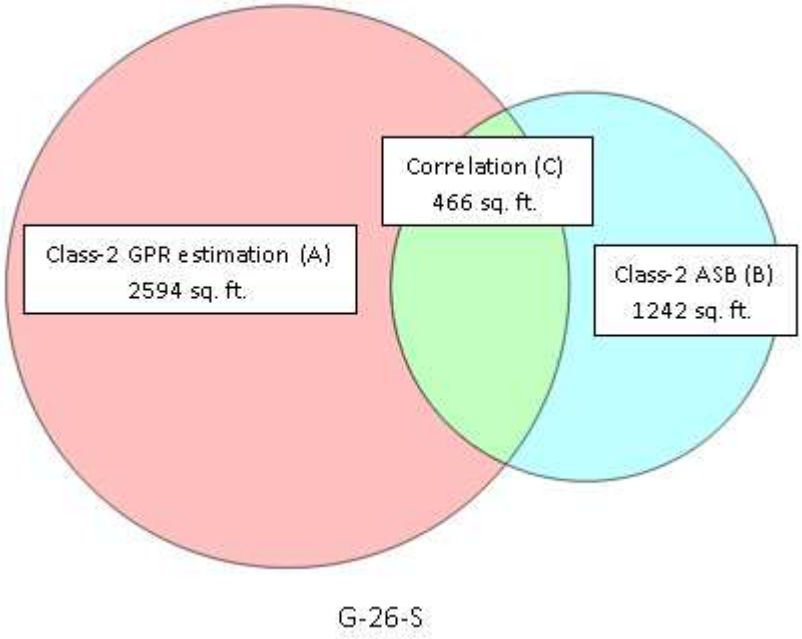

Figure 12: Comparison of G-26-S class-2 data

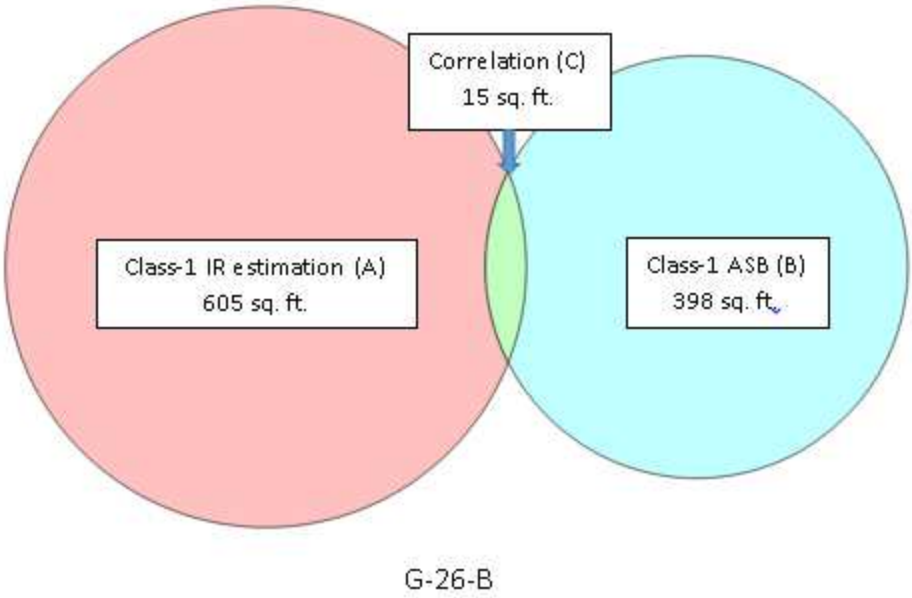

Figure 13: Comparison of G-26-B class-1 data

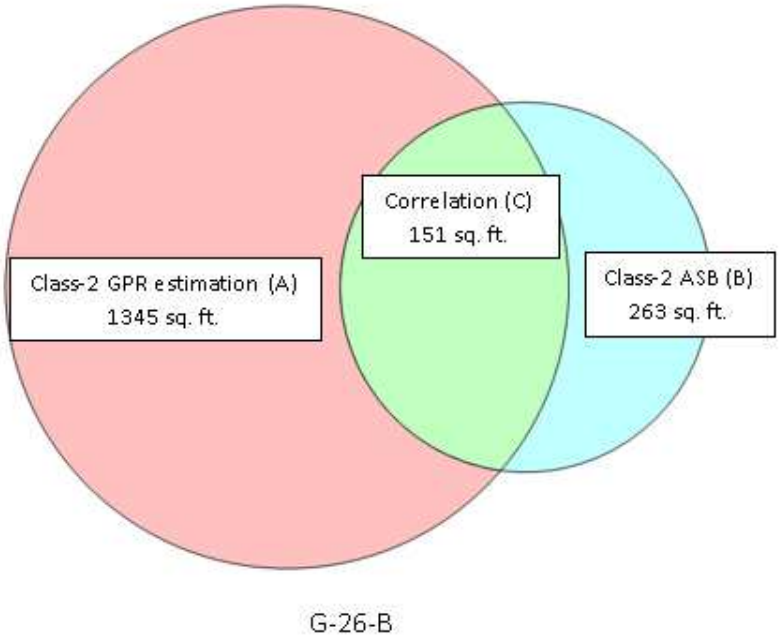

Figure 14: Comparison of G-26-B class-2 data

Table 8: Summary of estimated and rebuilt class-1 areas

Bridge	Estimated Class-1 areas using infrared	Class-1 As-Built area	Class-1 estimated areas correlating with ASB data	Accuracy of Infrared cameras for Class-1 areas
Units	%	%	%	%
G-26-U	5.4	7.58	8.69	43.82
G-26-T	9.39	6.71	4.05	59.34
G-26-S	3.70	4.89	2.27	43.62
G-26-B	6.99	10.63	2.55	40.30

Table 9: Summary of estimated and rebuilt class-2 areas

Bridge	Estimated class-2 repair work	Class-2 As-built repair work	Accuracy of GPR in detectable areas	Percentage of class-2 As-Built data undetectable	Percentage of as-built area correlating	Percentage of undetectable area rebuilt as Class-2
Units	%	%	%	%	%	%
G-26-U	15.4	1.89	90.08	7.91	2.81	7.73
G-26-T	8.69	4.27	77.88	36.12	9.53	79.14
G-26-S	32.80	15.70	84.38	23.8	49.27	48.12
G-26-B	10.69	4.63	90.64	41.44	70.65	68.85

4.3 Data Assessment

The assessment is first made on a case-by-case basis for each deck followed by more general assessment from looking at all four decks together.

4.3.1 Assessment of data from each bridge deck

4.3.1.1 G-26-U

Bridge G-26-U is located at milepost 416.541 on I-70. This bridge was built in 1970. The surface area of this deck is 8736 sq. ft. The NBI (National Bridge Index) deck rating and deck element condition state of this deck are 5 and 1 respectively. The element condition rating means that the deck has no spalling or delaminated areas. A NBI deck rating of 5 is given to decks in

fair condition state. Fair condition state is assigned to decks with heavy scaling of up to 1”, spalling of up to 5% of deck area, deterioration and water saturation of 20-40% of deck area, considerable leaching, and partial depth failures.

The repairs estimated in percentage of total deck area by GPR, IR and visual inspections are 6.4% class-1, 15.7% class-2 and 2.2% class-3. The total deterioration is estimated to be 24% of total deck area i.e. NBI deck rating = 4. The average asphalt cover and concrete cover over the top reinforcement as calculated using GPR are 2.9 in. and 3.4 in. respectively.

The following information is available about the status of deck joints from a report by Infrasense. The compression joint of the deck are in condition state of 3 (poor condition). 84 ft. of pier joints is in condition state 2 (fair condition) and 84 ft.is in condition state 3 (fair condition).

Figure 15 and figure 16 are plots showing as-built data along with the overlays of estimated repair work on the deck area for class-1 and class-2 respectively. The calculated as-built data of class-1 repair is 662.26 Sq. ft., which is 7.5% of the total area. Only 8.7 % of this repaired area is correlates with the class-1 damage estimated by IR thermography.

The class-2 area estimated by GPR is 1345.35 sq. ft. i.e. 15.4% of the total deck area. The calculated as-built data for class-2 repair is 165.43 sq. ft., which is 1.8% of the total deck area. 2.6% of this area correlates with the estimated class-2 repair work by GPR. If we assume all the area detected by GPR as deteriorated it would still be inaccurate by 10.5%. According to the report provided by Infrasense research studies have shown that GPR repair quantities are within 3.5% of inaccuracy.

Figure 17 shows the overlay of GPR estimated class-2 damage on the contour map of the concrete cover. The contour map shows the areas of concrete cover ranging from 0 to 5 inches

with areas of higher cover in lighter yellow, and darker red for areas with smaller cover. The areas of higher cover were calculated to be approximately 375.73 sq. ft. by visually picking areas of highest cover, which is 4.3% of the total deck area. It is observed that of the 20% of total class-2 areas estimated by GPR fall in the areas of higher cover.

Figure 18 shows the overlay of GPR estimated class-2 on the contour map of asphalt thickness along with class-1 and class-2 as-built data. The asphalt thickness on the deck ranging from 0 in. to 5 in., the areas of higher thickness are represented in lighter green with increasing darkness to darker blue for minimum thickness. The areas of higher cover were calculated to be 6% of the total deck area using a similar procedure used on concrete cover maps. The deck has higher asphalt thickness on the fifth span from west and along the north extreme of the deck. It is also noted that 56.6% of estimated class-2 areas falls under areas of lighter color i.e. areas of higher asphalt thickness.

This means that about 76.6% of the area estimated using GPR is either under areas of higher concrete cover or higher thickness of asphalt or both.

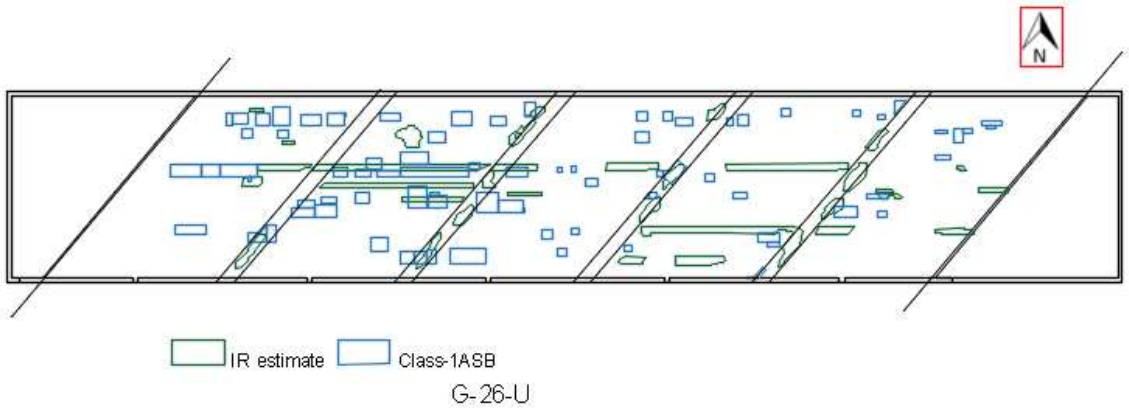

Figure 15: Class-1 estimation and as-built data on deck plan G-26-U

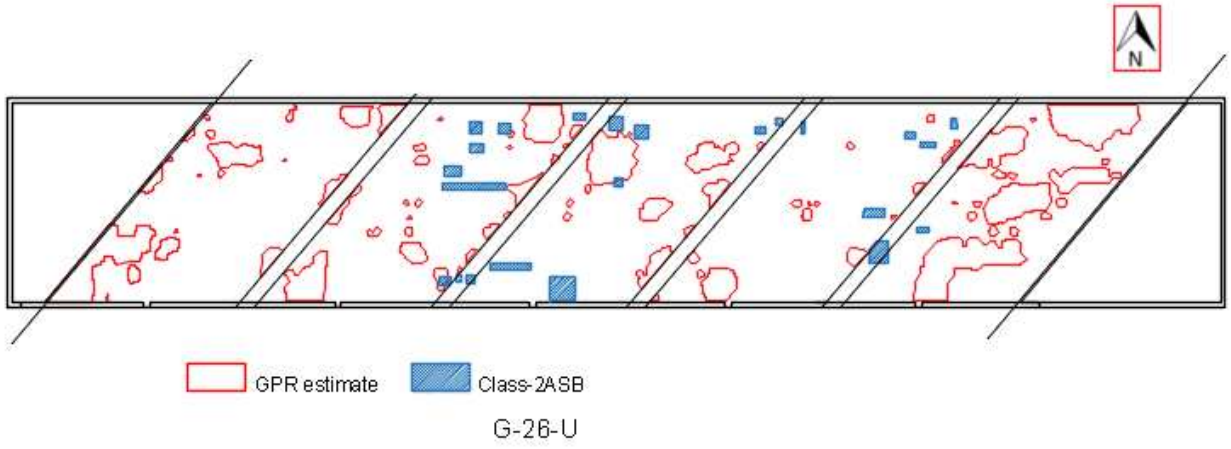

Figure 16: Class-2 estimation and as-built data on deck plan for G-26-U

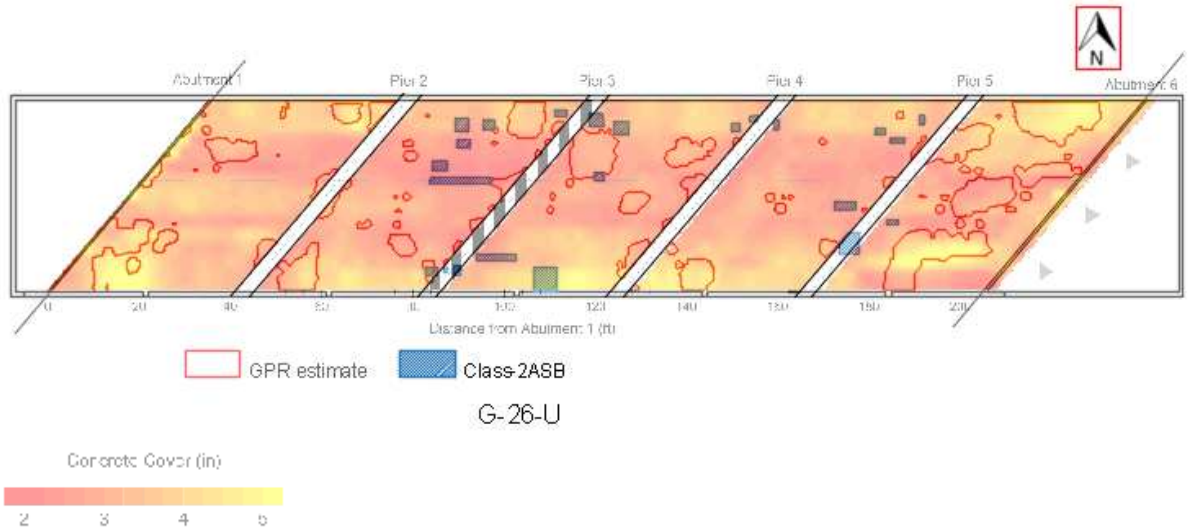

Figure 17: Contour map of concrete cover overlaid on deck plan with class-2 estimation and as-built data for G-26-U

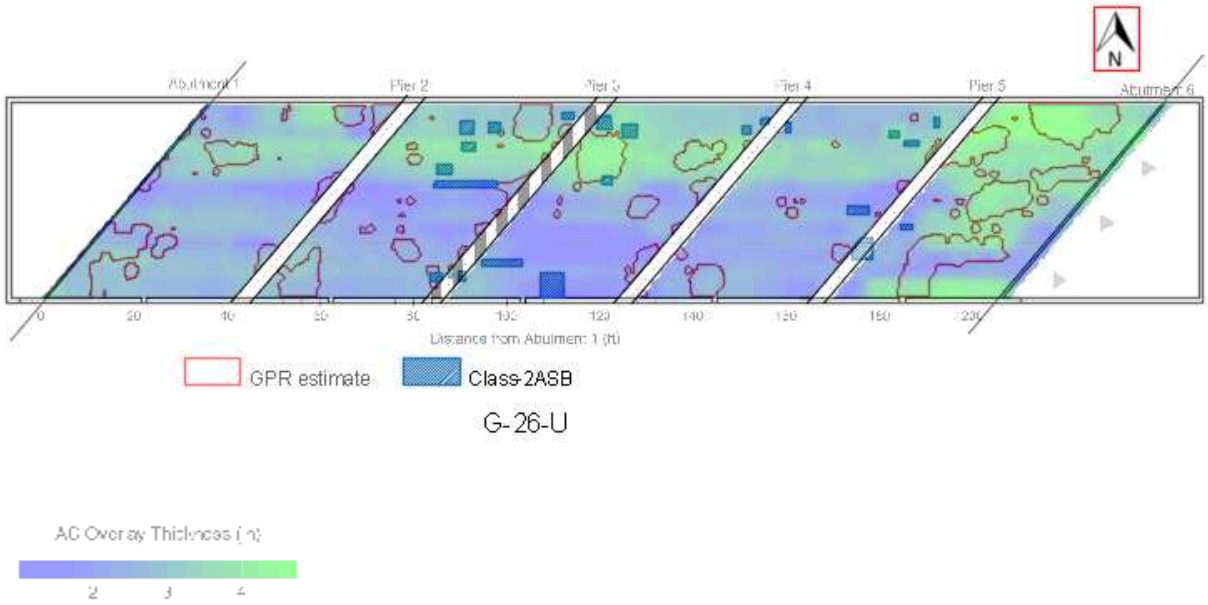

Figure 18: Contour map of asphalt cover overlaid on deck plan with class-2 estimation and as-built data for G-26-U

4.3.1.2 G-26-T

G-26-T is a bridge located at milepost 411.614 on I-70. The bridge deck is a concrete deck with asphalt overlay. This bridge was built in 1970. The NBI deck rating and deck element condition state of the deck are 7 and 1 respectively. A NBI rating of 7 is given to decks in good condition i.e. decks with sealable cracks, light scaling and no spalling. Element condition state 1 is for decks without surface spalling or patching.

The estimated repairs in percentage of total deck area by GPR, IR and visual inspections are 9.4 % of class-1, 8.7 %of class-2 and 1.1 of class-3. The average concrete cover and asphalt cover over the top reinforcement as calculated using GPR are 3.7 in. and 3.4 in. respectively.

The report by Infrasense has the following information about the deck joints. About 8 ft. of the joints are in condition state 2 (fair condition) and 95 ft. are in condition state 1 (good condition). The joints are filled with compression seal and asphalt has been pushed down into the joints between curbs and has minor leakage. The compression seals at the approach slabs are covered in asphalt.

Figure 19 and figure 20 are plots showing as-built data along with overlays of estimated repair work on the deck plan for class-1 and class-2 respectively. The estimated class-1 repairs by IR are 628.9 sq. ft. i.e. 10.59% of total deck area. The rebuilt class-1 areas are 398.54 sq. ft. i.e. 6.71% of the total deck area. In the rebuilt area only 16.18 sq. ft. correlates with the estimated repair work by IR, which is 4.06% of the repaired work.

The estimated class-2 area by GPR is 516.57 sq. ft. i.e. 8.7 % of total deck area. The calculated as-built area of class-2 repairs is 253.87 sq. ft., which is 4.2% of the deck area. In class-2 as-built data 15.46 sq. ft. correlates with the estimated area i.e. 6.09% of total estimated area. If the area estimated by GPR is assumed to be 100% deteriorated the GPR estimation will be 77.88 % accurate for detectable area.

It is observed that 115.87 sq. ft. of the deck area falls in area that was not detectable with GPR i.e. 1.95% of the total deck area but 36.12% of the class-2 repair work. 79.14 % of the areas undetectable at the expansion joints have been rebuilt as class-2. There is no class-1 rebuild work in the areas undetectable near the expansion joints.

Figure 21 shows the overlay of GPR estimated class-2 damage on the contour map of the concrete cover. The contour map shows the areas of concrete cover ranging from 0 in. to 5 in. lighter colors for areas with higher cover and darker colors for areas with lesser cover. The areas in green in the contour have cover of more than 5 in. They cover 195 sq. ft. of the total deck area

i.e. 3% of the total deck area. The areas that are in green are consistently falling under areas estimated as deteriorated by GPR except for two small contours of 6.8 sq. ft. of the total 195 sq. ft. green regions on the deck.

Figure 22 shows the overlay of asphalt thickness and estimated class-2 repair areas by GPR on the deck plan. The contour map shows areas of higher thickness in lighter green to areas of smaller cover in darker shades of blue. It is calculated that except for 21.6% of the total area estimated by GPR, the rest of it falls under either higher thickness of asphalt or higher concrete cover. The only area that correlates with sounding is near the south edge at the second joint from the west side of the bridge. This area is an area with lesser asphalt and concrete cover.

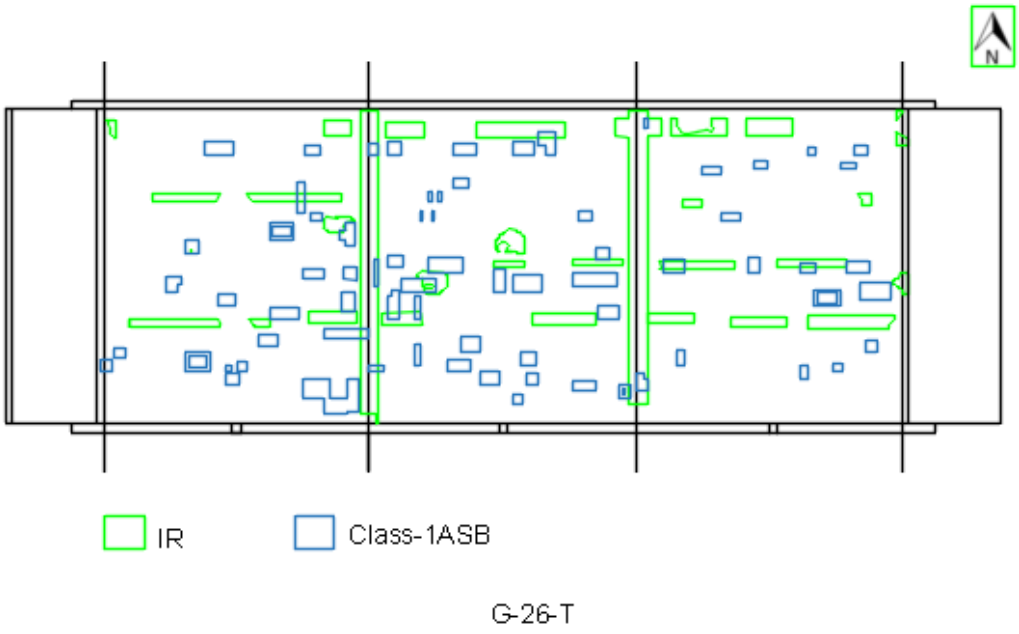

Figure 19: Class-1 estimation and as-built data on deck plan for G-26-T

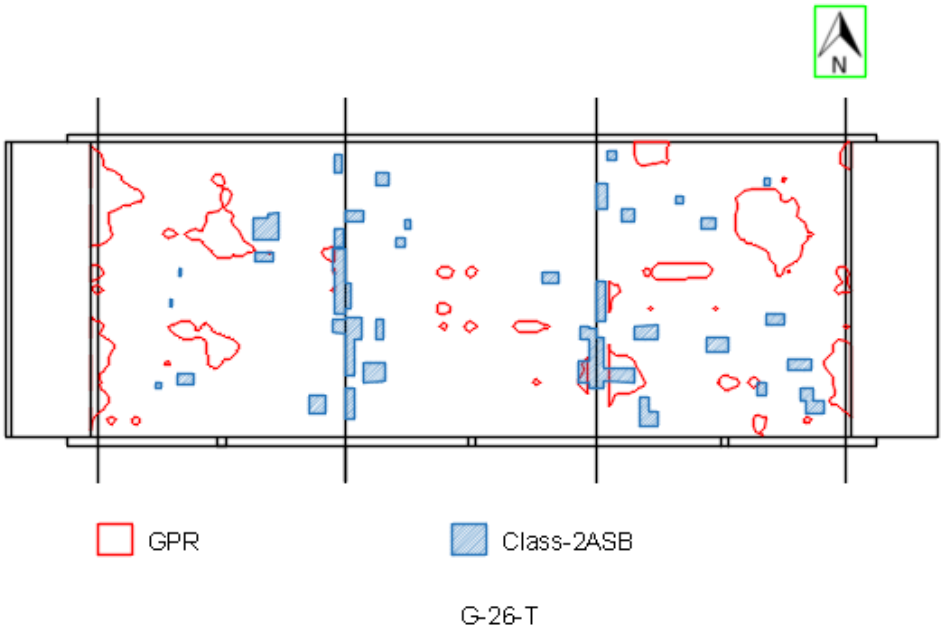

Figure 20: Classs-2 estimation and as-built data on deck plan for G-26-T

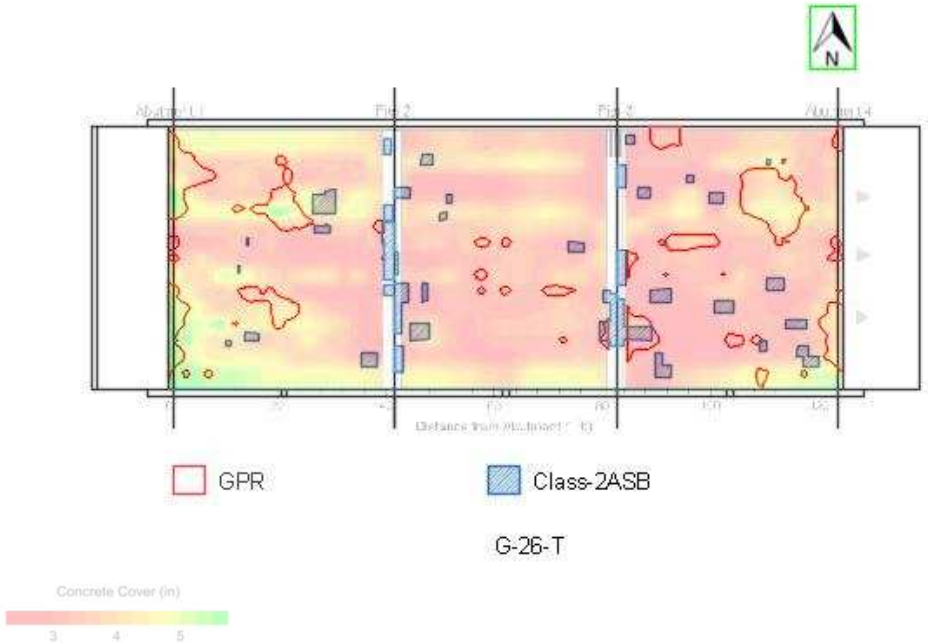

Figure 21: Contour map of concrete cover overlaid on deck plan with class-2 estimation and as-built data for G-26-T

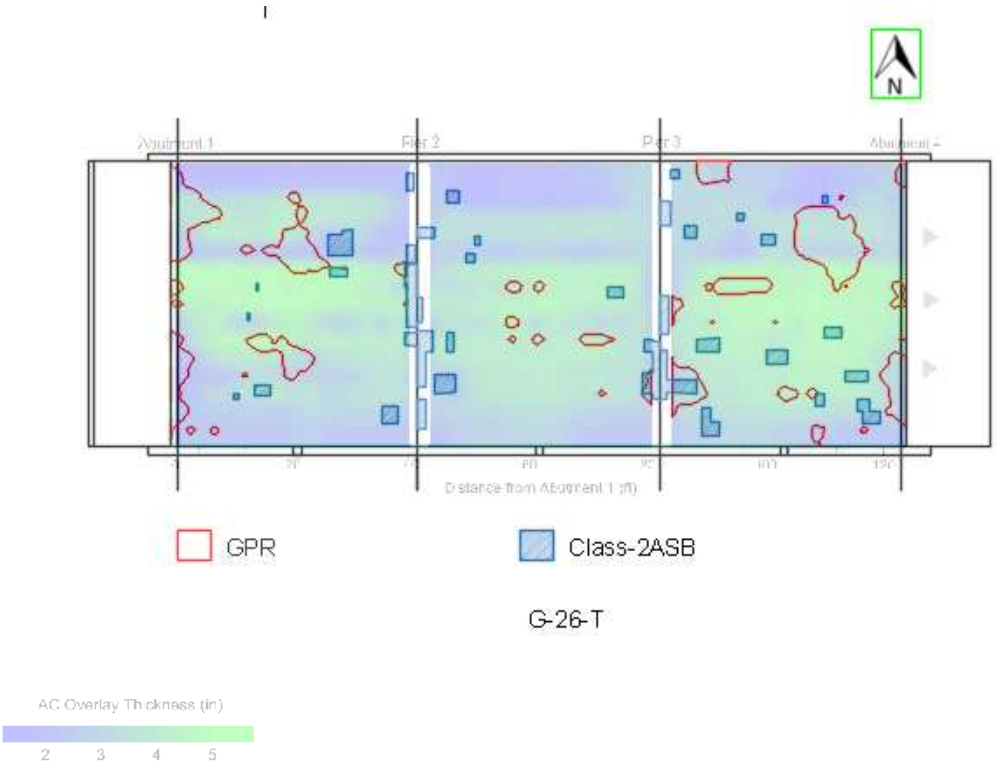

Figure 22: Contour map of asphalt cover overlaid on deck plan with class-2 estimation and as-built data for G-26-T

4.3.1.3 G-26-S

G-26-S is a bridge located at milepost 416.542 on I-70. The bridge deck is a concrete deck with asphalt overlay. The deck has a surface area of 7907.8 sq. ft. This bridge was built in 1965. The NBI deck rating and deck element condition state of the deck are 6 and 1 respectively. NBI rating 6 is given for decks in satisfactory condition i.e. decks with excessive amount of open cracks at more than 5 ft. interval and extensively deteriorated joints. Element condition state 1 is for decks without surface spalling or patching.

The estimated repairs by GPR, IR and Visual inspection in percentage of total deck area are 3.7% of class-1, 32.8% of class-2 and 1.6% of class-3. The average concrete cover and asphalt cover over the top reinforcement as calculated using GPR are 3.2 in. and 2.1 in.

respectively. These estimates means that GPR and IR suggest the deck to be in condition of 5 (fair condition) using the NBI deck rating index.

The report by Infrasense for this bridge deck has the following information about the deck joints. The deck joints are in condition state of 3 (poor condition) for 85 ft. and condition state of 1 (good condition) for 67 ft. The deck joints have poured sealant at the joints.

Figure 23 and figure 24 are plots showing as-built data along with overlays of estimated repair work on the deck plan for class-1 and class-2 respectively. The estimated class-1 repairs by IR are 292.16 sq. ft. i.e. 3.7% of total deck area. The rebuilt class-1 areas are 386.84 sq. ft. i.e. 4.89% of the total deck area. In the rebuilt area only 8.8 sq. ft. is correlating with the estimated repair work by IR, which is 2.27% of the repaired work.

The calculated as-built area of class-2 repairs is 2593.76 sq. ft., which is 32.8% of the deck area. In class-2 as-built data 466.07 sq. ft. correlates with the estimated area by GPR i.e. 49.27% of rebuilt class-2 area occurs in regions detectable to GPR correlates with class-2 estimation made by GPR. If the area estimated by GPR is assumed to be deteriorated, GPR estimation will be 84.38 % accurate.

It is observed that 615.33 Sq. ft. of deck area falls in area that was not detectable with GPR i.e. 7.78 % of the total deck area but 23.84 % of the class-2 repair work. 48.12 % of the areas undetectable at the expansion joints have been rebuilt as class-2. There is no class-1 rebuild work in the areas undetectable near the expansion joints.

Figure 25 is overlay of GPR estimated the class-2 damage on the contour map of the concrete cover. The contour map shows the areas of concrete cover ranging from 6 in. to 0 in. with lighter colors for areas with higher cover and darker colors for areas with lesser colors. The areas in lighter yellow in contour have cover of more than 6 in.

Figure 26 shows the overlay of asphalt thickness and estimated class-2 repair areas on the deck plan. The contour map shows areas of asphalt cover ranging from 3 in. to 0 in. with areas of higher thickness in lighter green shades to areas of smaller cover in darker shades of blue. There seems to be little deck area with higher thickness of asphalt but unlike the other decks with a 6 in. difference between the minimum and maximum cover this deck has a 3 in. difference between the extremities in cover.

Figure 26 shows that the majority of the deck is covered in asphalt of thickness around 3 in. there is minor portion of deck towards the south covered in lesser thickness of asphalt of about 1 in.. The GPR estimation partially or completely estimated most of the deteriorated regions.

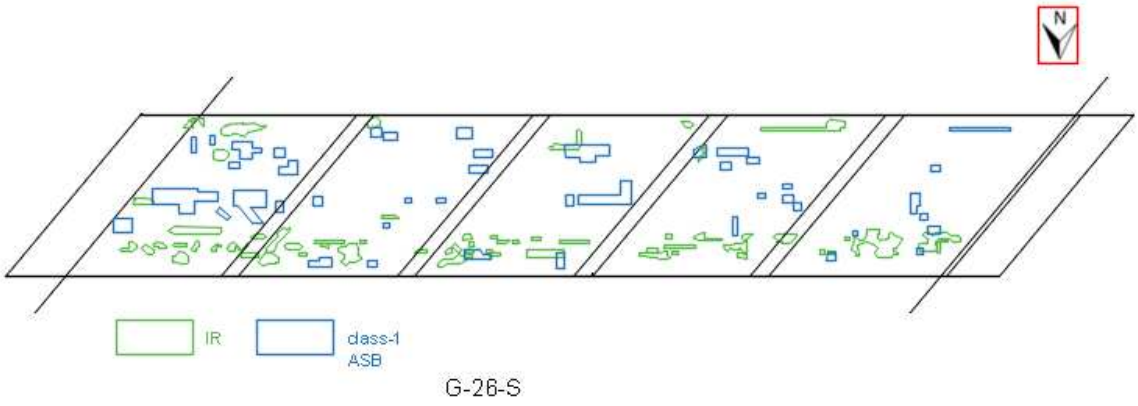

Figure 23: Class-1 estimation and as-built data on deck plan for G-26-S

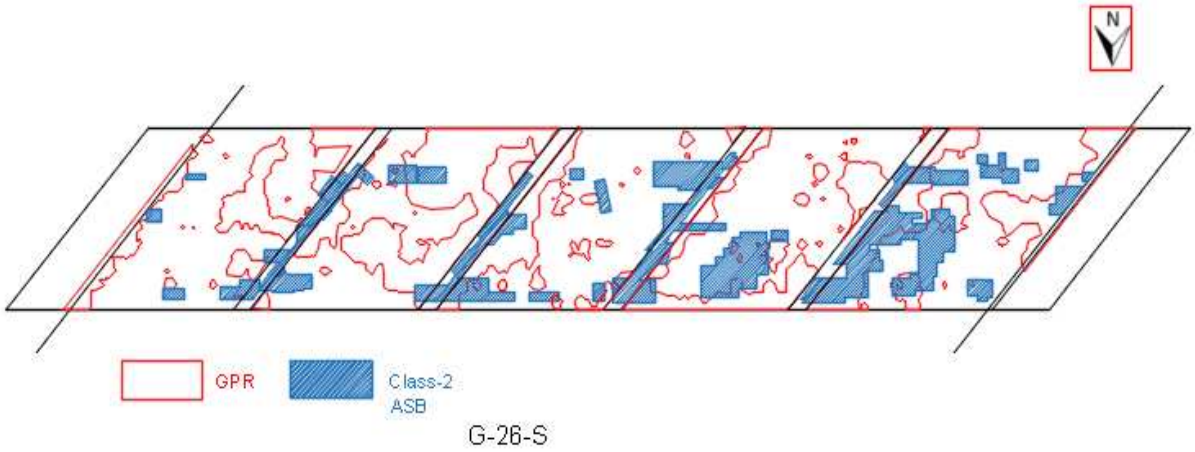

Figure 24: Class-2 estimation and as-built data for G-26-S

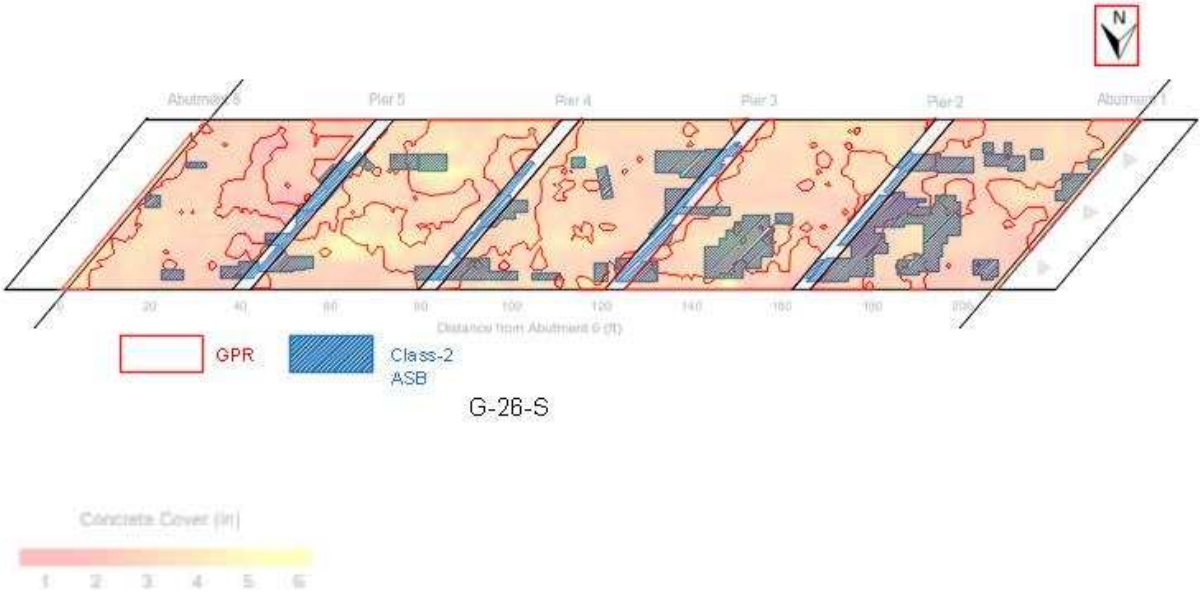

Figure 25: Contour map of concrete cover overlaid on deck plan with class-2 estimation and as-built data for G-26-S

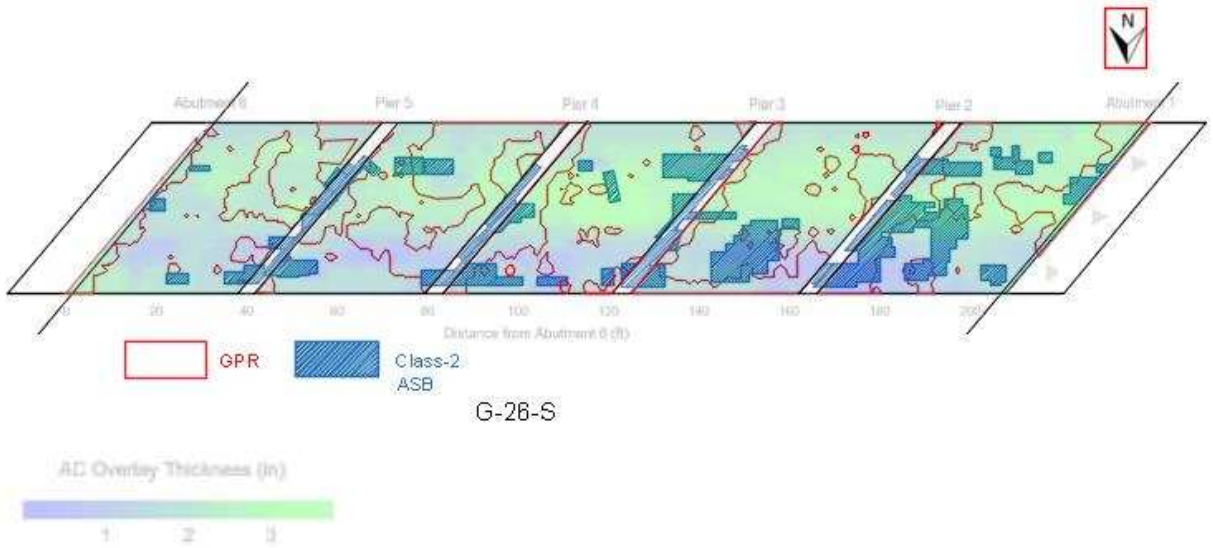

Figure 26: Contour map of asphalt cover overlaid on deck plan with class-2 estimation and as-built data for G-26-S

4.3.1.4 G-26-B

G-26-S is a bridge located at milepost 411.615 on I-70. The bridge deck is a concrete deck with asphalt overlay. The deck has a surface area of 5690.2 sq. ft. This bridge was built in 1964. The NBI deck rating and deck element condition state of the deck are 6 and 2 respectively. A NBI rating of 6 is given for decks in satisfactory condition i.e. decks with excessive amount of open cracks at more than 5 ft. interval and extensively deteriorated joints. Element condition state 2 is for decks with a combined distress of 2 % from repairs, spalls and delaminations.

The estimated repairs by GPR, IR and visual inspections in percentage of total deck area are 7.0 % of class-1, 10.7 % of class-2 and 2.3 % of class-3. The average concrete cover and asphalt cover over the top reinforcement as calculated using GPR are 3.8 in. and 3.9 in. respectively. The estimated areas by GPR and IR suggest the deck to be in condition state of 5 (fair condition) in NBI deck rating index as the total deterioration is between 20-40 %.

Reports from 2013 about the bridge by Infrasense contain the following information about the bridge joints. The joints are in a condition state 2 (fair condition). The bridge joints have compression seal joints in them. The piers indicate that there has been leaking previously and there is active leaking along the shoulders at the time of inspection in 2013.

Figure 27 and figure 28 are plots showing as-built data along with overlays of estimated repair work on the deck plan for class-1 and class-2 respectively. The estimated class-1 repairs by IR are 398.31 sq. ft. i.e. 7 % of total deck area. The rebuilt class-1 areas are 605.36 sq. ft. i.e. 10.7% of the total deck area. In the rebuilt area only 15.45 Sq. ft. correlates with the estimated repair work, which is 2.55% of the repaired work. The calculated as-built area of class-2 repairs is 323.4 Sq. ft., which is 5.68% of the deck area. In class-2 as-built data 151.2 sq. ft. correlates with the estimated area i.e. 70.65% of rebuilt class-2 area is in detectable regions to GPR is correlating with GPR estimation.

It is also observed that 109.4 sq. ft. of deck area falls in areas that are not detectable with GPR i.e. 2.8% of the total deck area but 33.82% of the class-2 repair work. 68.84% of the areas undetectable at the expansion joints have been rebuilt as class-2. There is no class-1 rebuild work in the areas undetectable near the expansion joints.

Figure 29 is overlay of GPR estimated class-2 damage on the contour map of the concrete cover. The contour map shows the areas of concrete cover ranging from 6 in. to 0 in. with lighter colors for areas with higher cover and darker colors for areas with lesser colors. The areas in shades of green in contour have cover of more than 6 in. the color gradually reduces to darker blue for areas of minimum thickness.

Figure 30 shows the overlay of asphalt thickness and estimated class-2 repair areas on the deck plan. The contour map shows areas of higher thickness in lighter green to areas of smaller cover in darker shades of blue.

GPR estimations show good correlations with the as-built data. The extreme north side of the deck has regions of higher thickness of both asphalt and concrete. The overlays show that there are three patches of class-2 work outside the class-2 areas estimated using GPR. Two of them on the first span from east side fall in the area of higher asphalt and concrete thickness near the extreme northern region of the deck. The third patch in the second span from the east falls in an area of higher concrete cover towards the southern edge of the deck. Of the 2593.76 sq. ft. rebuilt only 20 sq. ft. of repair work falls in regions away from deck joints.

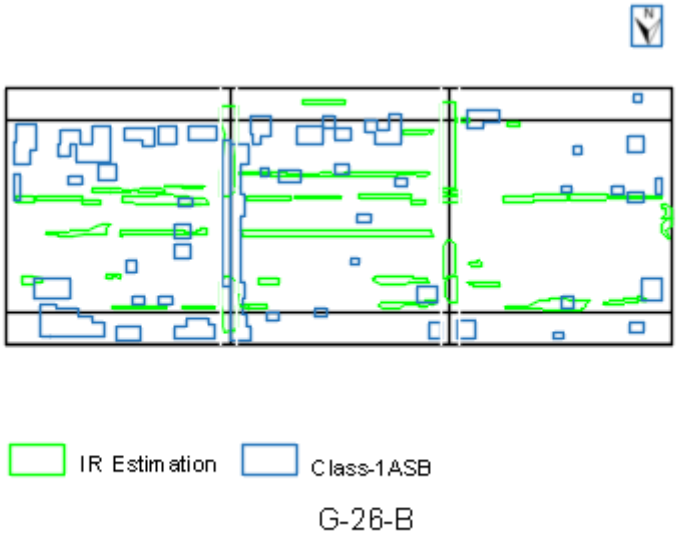

Figure 27: Class-1 estimation and as-built data on deck plan for G-26-B

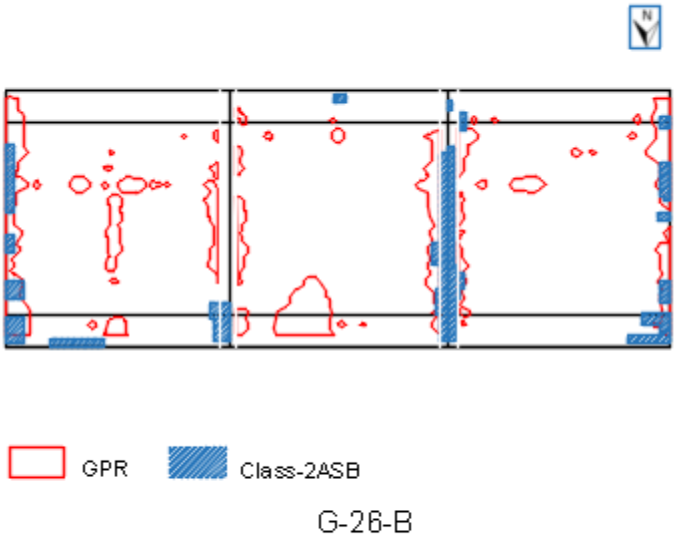

Figure 28: Class-2 estimation and as-built data on deck plan for G-26-B

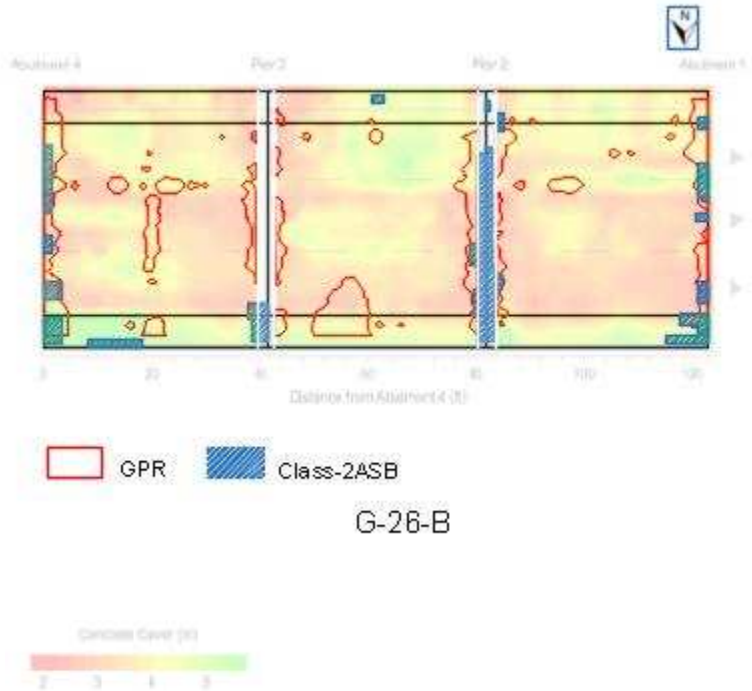

Figure 29: Contour map of concrete cover overlaid on deck plan with class-2 estimation and as-built data for G-26-B

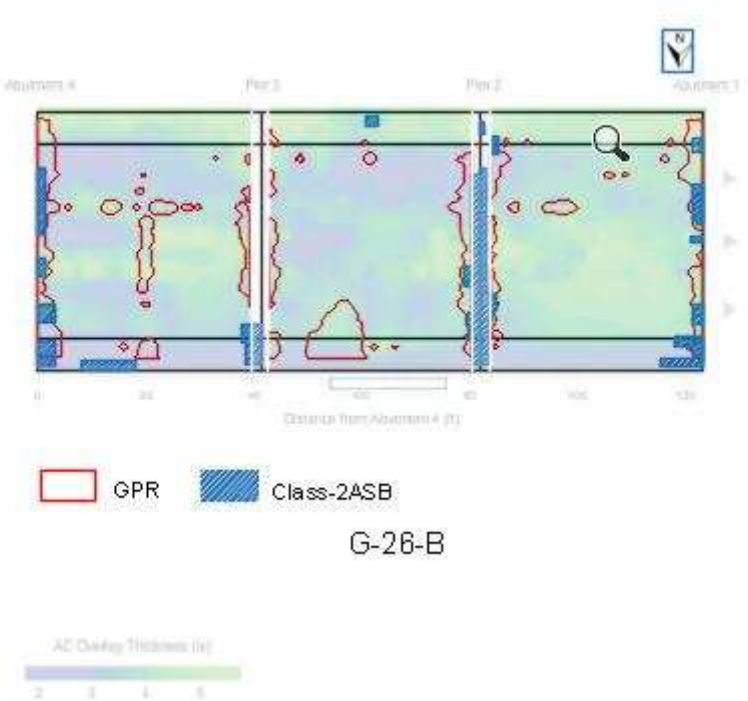

Figure 30: Contour map of asphalt cover overlaid on deck plan with class-2 estimation and as-built data for G-26-B

4.3.2 Assessment from the complete data set

The data shows that the area near the deck joints that is undetectable to GPR is more vulnerable to class-2 damage. The class-2 damage in undetectable regions averages to 65.7 % of the total undetectable area for G-26-T, G-26-B and G-26-S. G-26-U has only a damage of 7.73 % of total undetectable area. G-26-U has compression seal joints just like G-26-B and G-26-T. As the areas near joints seem to be vulnerable in Table 10 compares the element condition of the joints to the percentage of areas near the joints that are rebuilt.

The difference seems to be that the deck (G-26-U) is in a better condition than the other three decks judging by the total deteriorated area in as-built data. It is observed that deterioration at deck joints is indicated as class-1 in the scanning estimates, but there is no class-1 repair work at the deck joints for G-26-T, G-26-U and G-26-S. G-26-U has partial class-1 work at the joints.

Table 10: Element condition state and class-2 as-built data near the deck joints

Bridge	Joint type	Element condition state	Percentage of area at the joint rebuilt as class-2
G-26-U	Compression joint	3	7.73
G-26-T	Compression seal	8 ft. at state 2 and 95 ft. at state 1	79.14
G-26-S	Compression joint	67 ft.at state 1 and 95 ft. at state 3	48.12
G-26-B	Compression joint	2	68.85

There is poor correlation between the class-2 as-built data and the GPR predicted class-2 areas for G-26-U and G-26-T, with the GPR scans predicting only 2.81 % and 9.53 % of total rebuilt area. G-26-B and G-26-S show much better correlation when observed quantitatively. The correlating class-2 repair work predicted with GPR for G-26-B and G-26-S is 49.27 % and 70.65 % of the total rebuilt class-2 area. There are two differences that can be observed, from the data available, between the two sets of decks. One difference is that the as-built data from sounding and chipping indicate that G-26-U has a total of 9.47 % of deterioration and G-26-T has a total of 10.98 % deterioration. G-26-S and G-26-B have a relatively higher deterioration of 20.6% and 15.26 % respectively. The second difference is that the areas detected by GPR for G-26-U and G-26-T are falling under areas of higher asphalt or concrete cover i.e. 76.6 %and 79.4 % of total estimated area by GPR. A similar occurrence has not been observed for G-26-S and G-26-B.

The possibility of the estimations being influenced by the change in average cover thickness is also looked into using the available data. Table 11 compares cover thickness to correlating AS-built areas considering that GPR estimation is related to energy loss in waves which is dependent on deck thickness (refer section 2.3.2.2). Figure 31 is a plot of the concrete cover, asphalt cover and total cover compared to class-2 correlation.

Table 11: Cover on rebar and percentage of as-built data correlating with GPR

Bridge	Concrete cover	Asphalt cover	Total cover	AS-built class-2 data correlating with GPR
Units	in.	in.	in.	%
G-26-U	3.4	2.9	6.3	2.81
G-26-T	3.7	3.4	7.1	9.53
G-26-S	3.2	2.1	5.3	49.27
G-26-B	3.8	3.9	7.7	70.65

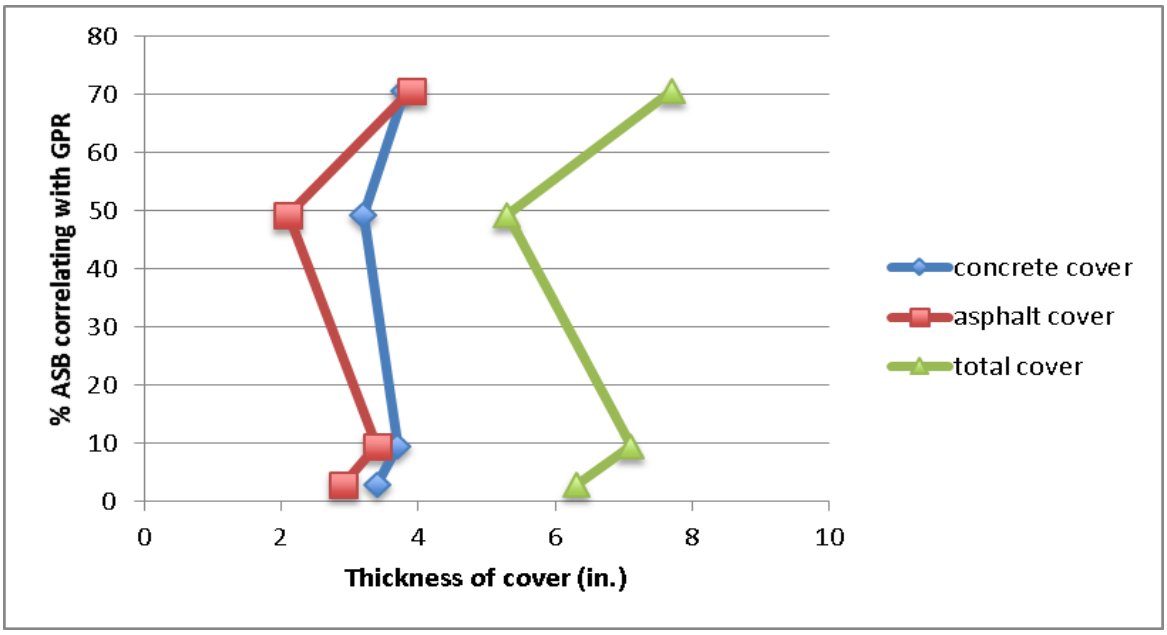

Figure 31: Plot of cover thickness and as-built correlation percentage

4.4 Inference from assessment of data

4.4.1 Infrared Thermography

IR thermography did not show correlation of more than 8.7 % to the as-built data in any of the cases for class-1 deterioration. Even when assumed that areas detected by IR as 100 % deteriorated the average accuracy of the IR on the 4 decks is 46.77 % with the highest accuracy being 59.34 % for total class-1 area. It is possible that asphalt overlay on the deck is weakening

the ability of infrared camera to capture the temperature differentials occurring below the asphalt overlay.

Data regarding the areas detected by infrared cameras as deteriorated and not correlating with class-1 rebuilt area is not available. It is possible that the areas could still be deteriorated or the temperature differentials indicated by the deck surface could be due to a characteristic of the asphalt overlay like debonding. Comparing the infrared thermography estimation to the class-1 deterioration on decks without asphalt overlay could help us understand the extent to which the asphalt overlay is affecting the data.

The estimations from infrared thermography have been important in determining the deteriorated areas near the deck joints that are not accessible for GPR scanning. The estimations from these areas are important as the areas seem to be more vulnerable to deterioration as mentioned in section 4.3.2. 7.91 % (G-26-U), 36.12 % (G-26-T), 23.8 % (G-26-S), and 41.44 % (G-26-T) of the total rebuilt class-2 areas in each deck fall in the areas not accessible to GPR. These class-2 as-built areas show consistent correlation with infrared scanning. A possible inference is that the deteriorated areas in the areas near joints are usually class-2. Estimating such areas as class-2 repair shall improve the accuracy of estimations.

4.4.2 GPR scanning

As observed decks G-26-U and G-26-T do not show much correlation between GPR scans and as-built data. The GPR estimations for class-2 areas on G-26-U and G-26-T fall on the areas with larger cover on the reinforcement. Which means the GPR waves are losing more energy in the areas with higher cover for these decks. There are two possible causes for wave attenuation in such regions. The areas could have deterioration that was not detectable to sounding or it is possible that the wave attenuation is related to the higher cover.

The forms of deterioration that cannot be detected by sounding but can be detected by GPR are corrosion, higher chloride content, and cracking that has not propagated to an advanced stage. The deterioration that can be detected by sounding and not detected by GPR radar are areas that have delaminations/cracks but do not have a corrosive environment such as chloride content or moisture etc. If we make a hypothesis that the GPR has detected all of the areas that have corrosive environments and sounding has detected all the areas with delaminations/cracks in advanced stages. This would mean that out of the four decks we have studied two decks that have only 2.81 % (G-26-U) and 9.53 % (G-26-T) of delaminated/cracked areas that are either caused from corrosion or have corrosive environments. This would also mean that 99.7 % (G-26-U) and 97 % (G-26-T) of the areas with corrosive environments have not led to any delaminations/cracks that are in advanced stage. This hypothesis is highly unlikely considering the fact that delminations/cracks are initiated by internal stresses that usually occur from the expansion of rebars due to corrosion.

Figure 32 is extracted from (Barnes & Frogeron, 2008), this figure has 32,768 reflection wave amplitudes from a single bridge deck. The assumption is that the maximum wave amplitudes are from regions that have minimum chloride content. The two-way travel time is a function of reflecting bodies. The reflecting body is the top reinforcement or bottom of the deck based on the data processing method used, and for thicker regions in the deck the waves take longer time to reach the antenna receiver. It can be seen that there is a decreasing trend of wave amplitude for increase in travel time. It is because the waves also loose energy when they travel through a higher cover over the reinforcement. An alternative hypothesis is that the wave attenuation in the GPR data has occurred due to the higher cover. The hypothesis is supported by

the overlays shown also indicate that the GPR estimation is coinciding with areas of higher cover.

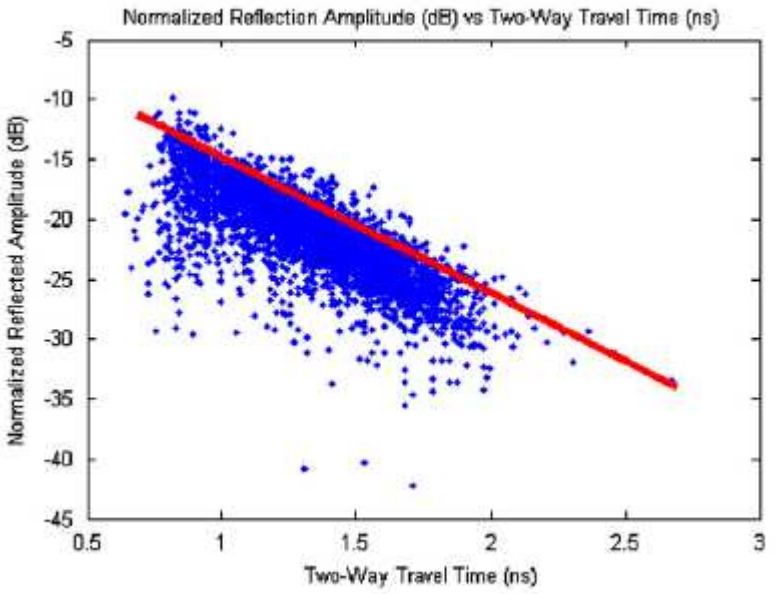

Figure 32: Normalized reflection amplitude vs two-way travel time (Barnes & Frogeron, 2008)

The GPR estimation on the four decks in this study was conducted with a procedure called depth correction, described by (Barnes & Frogeron, 2008) Initially, GPR estimation involved determining deteriorated regions using a threshold amplitude. The normalized wave amplitudes that are below maximum amplitudes by a certain threshold are considered deteriorated. ASTM suggests threshold amplitudes of 6-8 dB. This method did not show good correlation with sounding in some cases (Barnes & Frogeron, 2008). In such cases, the inaccuracy could be caused due to closer proximity of rebars than the mean rebar cover (Barnes & Frogeron, 2008). In this study by Barnes & Frogeron the researchers assumed that the deviation in data is from depth-amplitude relation and improved the data processing method by adding an additional step called depth-correction. Supporting their assumption that depth-amplitude relation is in fact the cause for wrong estimation from GPR. This means that the wrong estimation by GPR was due to

the closer proximity of rebars in certain areas than the mean rebar depth as the amplitudes in such areas fall below the threshold amplitudes in this case.

The depth correction procedure picks the 90th percentile amplitudes corresponding to each two-way travel time and assumes that the amplitudes above the 90th percentile are not influenced by deterioration. When not influenced by deterioration the amplitude variations are assumed to be caused only due to depth variations. The depth correction process applies regression analysis on the 90th percentile amplitudes to arrive at a more suitable common depth for the entire deck (Barnes & Frogeron, 2008). Using the corrected depth this procedure removes the depth dependent amplitude effects from the data and presents the data for a common corrected depth. The resulting plot between depth corrected reflection amplitude and two way travel time would be as shown in figure 33. The purpose of using depth correction procedure is to minimize the depth related errors on the deterioration estimation.

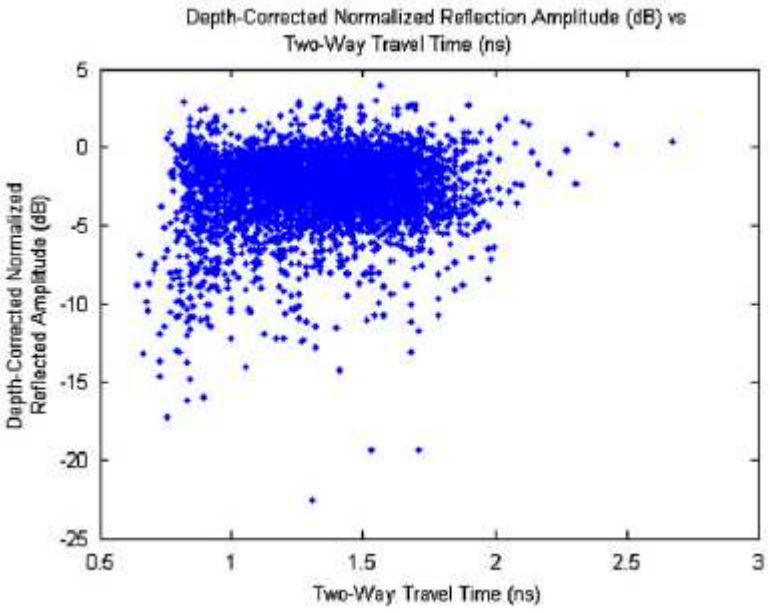

Figure 33: Depth correction normalized reflection amplitude vs two-way travel time (Barnes & Frogeron, 2008)

Accepting the hypothesis that the wave attenuation is caused by the higher cover on the decks. It means that even though the data is put through depth correction the corrected depth is still inappropriate for two decks (G-26-U and G-26-T) among four decks. A possible explanation is that the corrected depth is closer to regions with rebars at a closer proximity to the surface. When the amplitudes are adjusted to the corrected depth for picking deteriorated areas the amplitudes in the areas with higher cover are still falling below the selected threshold.

Using Figure 31, we also attempted to understand if there is any possible relation between accuracy and depth. Even though this plot does not seem to indicate any such relation we cannot make conclusions about existence or inexistence of any such relation when the depths selected for depth correction seem to be the issue for these decks.

Apart from estimating the areas with higher depth as deteriorated, selecting the wrong depth could result in different peak amplitudes. Having different peak amplitudes estimate different regions as deteriorated than the areas that should have been estimated as deteriorated in theory. It is also possible that in cases the when the selected depth is not appropriate for regions with least covers the GPR waves in such regions might not attenuate enough to detect deteriorated portions in those areas. Rebuilding decks to wrong estimation can lead to critical consequences to both safety of drivers and the design life of the bridge. Hence, there is a need to improve the interpretation technique from GPR data. In this study, we propose an additional step for data processing to improve interpretation through segmentation of the deck area. This procedure is explained in detail in chapter 5.

5. IMPROVED INTERPRETATION OF GPR DATA THROUGH DECK SEGMENTATION AND CORING STRATEGY

5.1 Deck Segmentation

Section 4.4.2 hypothesizes the possible causes of wave attenuation and examine each hypothesis. The areas that have higher cover than the cover used in depth correction seem to be the cause for wave attenuation in decks G-26-U and G-26-T. The GPR data seems to have more potential to estimate areas of deterioration if depth related wave attenuation can be solved.

This study proposes a newer method for improved interpretation of GPR data through segmentation of the deck area. This procedure can be carried out after developing a rebar cover contour for the entire deck area. Following is a step-by-step procedure for improved interpretation of GPR data through segmentation with an example. The example used to explain this procedure is deck G-26-T

Step-1: Divide the rebar cover and asphalt cover on the entire deck area into three intervals the areas with cover near the higher extreme, areas with moderate cover, and areas with less cover. In this case for deck G-26-T, the deck area is split into areas with cover of 3 in. and less, areas with cover of around 4 in. and areas with cover over 5in.

This division can also be made for 3 equal intervals between maximum and minimum cover. This could be more effective than the intervals we used in this example. With the data available to us it is not possible to pick areas in each cover interval. So in this example the fore mentioned intervals used.

Step-2: The entire deck is separated laterally and longitudinally to have the entire deck area segmented. The separations are planned in such a way that the segments are approximately the size of smaller contours. The longitudinal separation should be made for each pass of the GPR.

Separating deck area along the passes makes it easier to select the amplitudes in each longitudinal segment. The passes can further be split into equal intervals using the width of the smaller contours as reference.

The lateral separation can be decided similarly based on the width of smaller contours. The deck is split laterally at equal intervals. The offset from the west abutment of the deck is used as reference to identify each separation.

Figure 34 is bridge deck G-26-T separated longitudinally and laterally using the procedure explained above. The longitudinal separation is made for each pass. The passes are split into half the width again because some contours are less than half the size of each pass. The lateral separation is made at intervals of 5 ft. Each segment can be identified using the southwest co-ordinate on each segment. For example the co-ordinate for southwestern most segment of the deck is (0,0), the subsequent segments to the east of this segment are (0,5), (0,10), (0,15) and so on. The segments to the north of (0,0) would be (1,0), (2,0) so on. The nomenclature in general form (longitudinal separation number to the south of segment, offset of western end of the segment from western abutment).

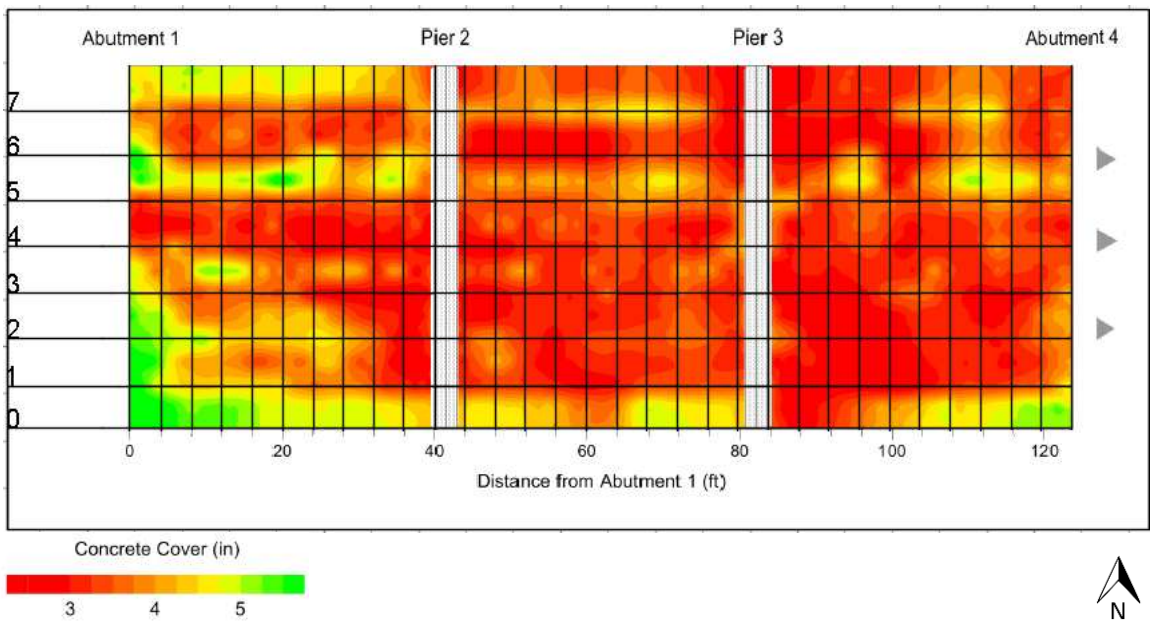

Figure 34: Segmented surface area of deck-G-26-T with contour map of asphalt overlay

Step-3: Separate the segments of the deck area into respective interval of concrete cover from step-1. When some segments seem to be partially having covers in both intervals such areas can be put in a cover interval that covers the majority of the segment. When we separate the amplitudes from areas in each interval we get three sets of data.

To explain step-3 through an example, the segments on the southernmost side of the deck are used. In table 12 the southernmost segments of deck G-26-T are separated to corresponding category of thickness.

Step-4: In this step we select the areas in each interval from step-3 and split each of those areas into three different areas of asphalt cover. The output would be 9 sets of segmented areas for the entire deck and 9 sets for amplitudes. Each set of amplitudes are picked from each set of segments split to respective concrete cover. The asphalt cover separation is carried out on each set of concrete cover separately as concrete and asphalt are two different materials that would have different di-electricity and different response to GPR waves. Hence, the total cover from asphalt and concrete cover cannot be added together for a common segmentation procedure.

Figure 35 is segmented asphalt deck plan of G-26-T with the contour map of asphalt overlay. In table 12 the segments selected in step-3 are further subcategorized into respective asphalt cover categories as explained in step-4.

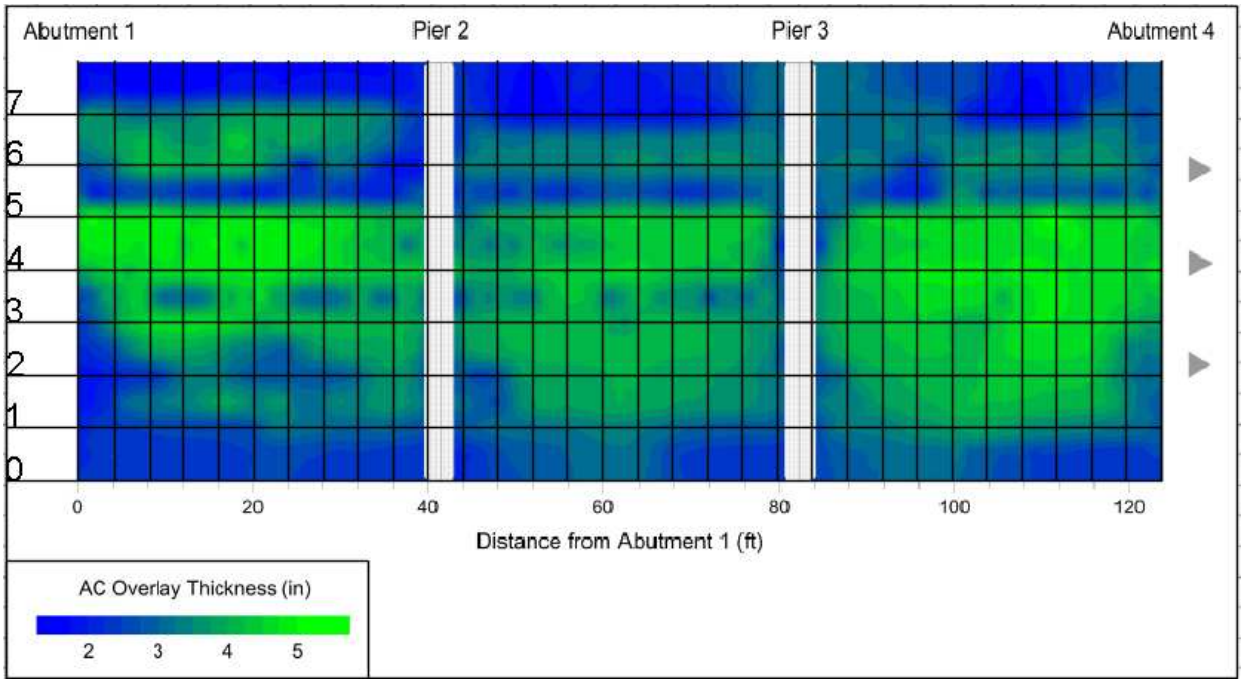

Figure 35: Segmented surface area of deck G-26-T with contour map of asphalt overlay

Table 12: Categorizing the southernmost segments of deck on G-26-T into respective cover categories

Segments	Concrete cover			Asphalt cover		
	Highest	Moderate	least	Highest	Moderate	Least
0,0	X					X
0,5	X					X
0,10	X					X
0,15	X					X
0,20		X				X
0,25		X				X
0,30		X				X
0,35		X				X
0,40		X				X
0,45		X				X
0,50		X			X	
0,55		X			X	
0,60		X			X	
0,65		X			X	

0,70		X			X	
0,75		X				X
0,80		X				X
0,85			X			X
0,90			X		X	
0,95			X		X	
0,100		X			X	
0,105		X				X
0,110			X			X
0,115			X			X
0,120			X			X

The 9 sets of data categories selected using table 13 is represented in the form of matrix in table 14.

Table 13: 9 sets of amplitude data separated using table 12

	High concrete cover	Medium concrete cover	Less concrete cover
High asphalt cover	x	x	x
Medium asphalt cover	x	x	x
Low asphalt cover	x	x	x

Step-5: The depth correction process will be carried out on each set of data separately. The output would be 9 different depths for each of segmented areas.

The correlation that could be achieved through this procedure is unknown as this has not put this procedure into execution. The correlation could be at least as good as the correlation achieved for decks G-26-B and G-26-S. Since these decks had similar covers with different distribution through the deck area and the depth correction procedure was sufficient to achieve a correlation for GPR with sounding and chipping.

The sure way to know if our hypothesis is true is if we put the GPR data through this procedure and compare the outcome to the as-built data. It is possible that wave attenuation in

these areas can also be caused by other factors. To further understand the factors that are influencing wave attenuation this study proposes a coring strategy. This strategy also covers the data unavailable for this study to allow future research to collect similar data before the decks are rebuilt.

5.2 Coring strategy

The primary objective of proposing this strategy is to understand if there are any additional contributions to wave attenuation when holding the hypothesis that wave attenuation in cases such as G-26-U and G-26-T is caused by higher depth cover. This sections also enlists the expectation from each core when the waves are not influenced by depth correction i.e. when the depth-amplitude relation is completely removed. Studying these cores in detail and comparing the cores to similar cores with lesser wave attenuation will allow us to understand additional contributing factors to wave attenuation.

Strategy for picking cores:

Reference cores: Reference cores must be taken from regions that are not falling under areas estimated by GPR or sounding and chipping. These cores will serve as reference for the di-electricity of concrete in areas that are in good condition. Reference cores must be taken from areas of different concrete covers to compare with deteriorated cores with similar covers.

Core type 1: cores from areas that are estimated by Infrared thermography as class-1 that are not correlating with sounding. Ideally, these areas still have delamination that has not been detected by sounding. If the case is otherwise it is possible that the infrared thermography has been influenced by asphalt cover.

Core type 2: cores from areas with a cover close to the mean cover that are estimated as class-2 that correlate with sounding. Ideally, these cores would have an increased di-electricity or they

have cracks in early stages. If the peak amplitudes are miscalculated from using wrong depth for depth correction these cores could still have relatively high di-electricity than cores with similar covers in reference cores.

Core type 3: Areas that are estimated by GPR as class-2 but fall under areas of highest (region 3) concrete cover. Ideally, we must see results similar to region 2. In cases where the depth used is inappropriate the GPR estimation could show these areas as deteriorated even when there is no deterioration as the amplitudes of waves reflected from these areas could be less than the threshold amplitudes calculated from a common depth after depth correction. The inappropriate depth would be a depth less than the depth of rebars in these areas.

Core type 4: Cores from areas with least cover estimated by sounding as class-2. Ideally these regions must have deterioration with no corrosive environment. If such cores are estimated by GPR as not deteriorated when there is an increased di-electricity due to corrosive environment it implies that the waves reflected have not attenuated enough when using threshold amplitudes calculated using an inappropriate depth after depth correction. The inappropriate depth would be a depth greater than the depth of rebars ion these areas

6. CONCLUSIONS AND RECOMMENDATIONS

6.1 Summary

Literature on a wide variety of topics related to bridge evaluations and NDE of bridge decks was studied to understand the challenges in evaluating bridges, the importance of evaluating bridge decks, the techniques at our disposal and the importance of addressing the requirement to improve evaluation techniques. For a country that has bridges with average age of 42 years and life expectancy of 50 years the need to adapt to a faster and more reliable technique than sounding and chipping seemed immediate for the USA. There are a wide number of alternative NDE techniques such as GPR, Impact echo, IR thermography, half cell-potential etc.

A large amount of literature on the NDE techniques was focused on the types of anomalies each NDE method can detect and the accuracy of each of these methods. This paper was directed on understanding and improving GPR and IR thermography as these are the techniques that CDOT is considering to adopt for bridge deck evaluation about the predicted bridge deck condition and the actual repaired areas are put together the observations from CDOT's decks did not seem to produce the levels of accuracy achieved in the earlier literature.

All the four decks used in this study had asphalt overlay. It is understood from the literature study that asphalt overlay could limit the ability of IR thermography to estimate class-1 deterioration. This study showed that IR thermography is very important in evaluating the areas near the expansion joints that are not accessible to GPR. The evaluation estimated these areas as class-1 regions. This study shows that estimating these areas as class-2 is more appropriate because majority of class-2 regions fall in these areas and these areas are usually class-2.

The class-2 estimation data by GPR for two (G-26-U and G-26-T) of the four decks did not correlate with as-built data from sounding and chipping. This study compared the data available from the two decks that did not correlate with the decks that did correlate (G-26-S and G25-B) to understand the possible cause for the data not to correlate. The comparison showed that the GPR estimation fell in areas of greater cover of asphalt or concrete for decks that did not correlate with sounding. From observations made from the data, the study moved forward by making a hypothesis that the wave attenuation was caused by thicker cover.

The hypothesis seemed to be the probable cause for wave attenuation in the decks after examining the alternative cases of wave attenuation. So this study proposed an additional step in the data processing method to minimize the depth-amplitude effect in the data through segmentation. In this procedure, we segment the deck area based on the size of smaller contours. Segmenting the deck area and separating areas that have similar cover into different categories. Processing the amplitude data of segments under similar categories separately minimizes the depth-amplitude relation in the data.

This study also suggests a coring strategy for future research in this direction. To collect more data for better understanding of the factors causing GPR wave attenuation in concrete.

6.2 IR Thermography Conclusions

- IR thermography is still important even when not effective for decks with asphalt overlay as they can be used to detect deterioration in areas not accessible to GPR.
- This study also shows that deterioration estimated through IR thermography near deck joint is more likely to be class-2. Estimating such areas as class-2 deterioration shall improve the accuracy of estimations.

6.3 GPR conclusions

- The GPR technology is the only type of NDE that can detect deterioration in asphalt covered bridge decks. Any judgment by CDOT on continuing to use the technology or not should be made only once the complete potential of this technology is achieved. The future research can be directed towards achieving the complete potential of GPR to take advantage of the abilities of this technology.
- The accuracy related research on GPR does not seem to have covered all types of bridge decks.
- Minimizing the depth-amplitude relation in previous research has shown improved results. The decks used in this study still seemed to be influenced by the depth-amplitude relation. Hence, the depth-amplitude relation in the data must be further minimized.
- Using improved interpretation through segmentation can possibly minimize the depth-amplitude relation in the GPR data. Minimizing depth-amplitude relation can improve the data interpretation from GPR scanning there by increasing the reliability of this technology.
- From the literature available on GPR it is understood that this technology is not appropriate for decks with cathodic protection. This is due to the interference of the cathodic protection with the GPR waves. If GPR is to be considered a long term solution alternatives to using cathodic protection must be considered.

6.4 Suggestions for future research

A huge repair backlog for bridges and a large number of bridges scheduled for repair in the coming years is also a huge research opportunity to improve bridge element evaluation

methods. This opportunity was used to advantage in this research. In a period of opportunity through this research we also place some meaningful suggestion for future research to improve evaluation of bridge decks.

- Scanning decks with asphalt overlay before and after removal of asphalt overlays with Infrared cameras can help us understand the extent to which asphalt overlay on decks influences the IR thermography data.
- In the future, taking notes and studying the asphalt overlay condition and concrete in areas detected by IR as deteriorated will give us more insight into thermal signatures of different anomalies.
- Developing software that can pick data from areas of different covers separately and process on its own. Such a development can completely eliminate depth-amplitude relations from the data.
- Studying wave attenuation from combinations of deterioration types at different depths can give us more insight into GPR wave attenuation from different anomalies. This would allow inspectors to produce reports with more detail on the probable deterioration.
- A limitation of using GPR is that it is not capable of detecting deterioration that does not have an increased di-electricity. Developing permeable solutions that can temporarily increase the di-electricity of delaminations/cracks that do not have corrosive environments could help solve the limitation of GPR of not being able to detect such deterioration.
- If GPR is considered a long term solution to evaluating bridge decks. Research should also be directed to understanding the influence of deicing salts on the wave attenuation and minimizing the deicing salt-amplitude relation.

- GPR is capable of detecting cracks in early stages unlike sounding that detects cracks in an advanced stage. GPR is additionally capable of detecting corrosion in rebars. Understanding the impact of repairing such areas on a deck life can help researchers reevaluate the current time intervals between which the decks are evaluated for deterioration. This could save resources of bridge owners significantly on the long run. The aforementioned time interval for evaluating decks can be arrived by evaluating sets of two decks in similar environment with similar loading after repairing each of the deck from a different evaluation method (GPR and sounding) between equal time periods.

WORKS CITED

1. AASHTO. (2011). *The manual for bridge evaluation* (2nd Edition ed.).
2. AASHTO. (2013). *Manual for Bridge Element Inspection* (1st Edition ed.).
3. ASCE. (2013). *Report card for America's infrastructure.* ASCE.
4. ASTM. (1997). *Standard Practice for Measuring Delaminations in Concrete Bridge Decks by Sounding.* American Society for Testing and Materials. ASTM.
5. ASTM. (2008). *Standard Test Method for Evaluating Asphalt-covered Concrete Bridge Deck Using Ground Penetrating Radar.* ASTM.
6. Barnes, C. L., & Frogeron, J.-F. T. (2008, March). Improved concrete bridge deck evaluation using GPR by accounting for signal depth-amplitude effects. *NDT&E International*.
7. Chen, R. H., & Scheff, J. J. (2000). Bridge Deck Inspection Using Chain Drag And Ground Penetrating Radar. *ASCE*.
8. D.Ciampa, J. (2009). *Non-Destructive Bridge Deck Test Using Ground Penetrating Radar.* Spectra Sub Surface Imaging, LLC.
9. Gucunski, N., Imani, A., Francisco, R., Nazarian, S., Yuan, D., Wiggenhauser, H., Kutrubes, D. (2011). *Non-destructive Testing to Identify Bridge Deck Deterioration.* Transportation Research Board.
10. Gucunski, N., Romero, F., Kruschwitz, S., Feldmann, R., & Parvardeh, H. (2011). *Comprehensive bridge deck detoriation mapping of nine bridges by Nondestructive evaluation technologies.* IOWA DOT. IOWA DOT.

11. Huston, D., Hu, J., Pelczarski, N., & Esser, B. (1999, september). Bridge deck evaluation with ground penetrating radar. *Second International workshop for Structural Health Monitoring.* Stanford University: University of Vermount.
12. INFRASENSE, Inc. (2014). *Nondestructive bridge deck condition evaluation.* Inspection report.
13. Lau, C. L. (1991, December). *Thickness estimation of subsurface layers in Asphalt Pavement.* Texas A&M UNiversity.
14. Lee, S., & Kalos, N. (2014). *Bridge inspection practices using non-destructive testing methods for concrete structure.* Construction Research Congress.
15. Love, B. (1986). *The Detection of Delamination in Reinforced Bridge Decks Using Infrared Thermography.* West Lafayette: Indiana Department of Highways Division of Resarch and Training.
16. Mark Moore, B. P. (2000). *Reliability of visual inspection for highway bridges Volume I: Final Report.*
17. Nawy, E. G. (2008). *Concrete Construction Engineering Handbook* (2nd ed.). CRC Press.
18. Rhazi, J. (2011, march). Test method for evaluating asphalt-covered concrete bridge decks using ground penetrating radar. *NDT&E International*.
19. Sagues, A. A., Moreno, E. I., Morris, W., & Andrade, C. (1997). *Carbonation in Concrete and Effect on steel Corrossion.* University of South Florida.
20. Scheff, J. J., & Chen, R. H. (2000). Bridge Decks Inspection Using Chain Drag and Ground Penetrating Radar.
21. Tonias, D. E. (1995). *Bridge Engineering.*

22. Vilbig, & Allen, R. (2014). *Air-Coupled and ground-coupled ground penetrating radar techniques.* Northeastern UNiversity.

23. Vittery, J., & Pearson-Kirk, D. (2008). Sulphate Induced Deterioration of Above Ground Components of Highway Structures. *Structural Faults and Repair*. Edinburgh, U.K.

24. Zachar, J., & Naik, T. R. (1991). *Principles of Infrared Thermography and Application for Assessment of Deterioration of the Bridge Deck at "Zoo Interchange"*. Milwaukee: University of Wisconsin.

APPENDIX A

Table A.1 Condition assessment methods and corresponding standards

Condition Assessment Method	Standards
Chain Dragging	(ASTM, 1997)ASTM D 4580-86
Chloride Concentration Testing	ASTM C 1218-99, AASHTO T 260-97, SHRP Product 2030
Coring	ASTM C 42-99, AASHTO T 24-02
Ground Penetrating Radar	ASTM D 6087-97, ASTM D 6432-99
Half-Cell Potential	ASTM C 876-91
Sounding	ASTM D 4580-86
Impact-Echo	ASTM C 1383-98a
Infrared Thermography	ASTM D 4788-88
Penetration Dyes	N/A
Petrographic Analysis	ASTM C 856-95
Rapid Chloride Permeability	ASTM C 1202-97, AASHTO T 277-96
Resistivity Testing	ASTM D 3633-98, ASTM D 6431-99
Skid Resistance	ASTM E 274-97,AASHTO T 242-96 ASTM E 303-93, AASHTO T 278-90
Ultrasonic Testing	ASTM E 494-95
Visual Inspection	N/A

Table A.2 Titles of inspection methods as specified in ASTM/AASHTO/SHRP

Standards	**Titles**
ASTM C 42-99	Standard Test Method for Obtaining and Testing Drilled Cores and Sawed Beams of Concrete
ASTM C 856-95	Standard Practice for Petrographic Examination of Hardened Concrete
ASTM C 876-91	Standard Test Method for Half-Cell Potentials of Uncoated Reinforcing Steel in Concrete
ASTM C 1202-97	Standard Test Method for Electrical Indication of Concrete's Ability to Resist Chloride Ion Penetration
ASTM C 1218-99	Standard Test Method for Water-Soluble Chloride in Mortar and Concrete

ASTM C 1383-98a	Standard Test Method for Measuring the P-Wave Speed and the Thickness of Concrete Plates Using the Impact-Echo Method
ASTM D 3633-98	Standard Test Method for Electrical Resistivity of Membrane-Pavement Systems
ASTM D 4580-86	Standard Practice for Measuring Delaminations in Concrete Bridge Decks by Sounding
ASTM D 4788-88	Standard Test Method for Detecting Delaminations in Bridge Decks Using Infrared Thermography
ASTM D 6087-97	Standard Test Method for Evaluating Asphalt-Covered Concrete Bridge Decks Using Ground Penetrating Radar
ASTM D 6431-99	Standard Guide for Using the Direct Current Resistivity Method for Subsurface Investigation
ASTM D 6432-99	Standard Guide for Using the Surface Ground Penetrating Radar Method for Subsurface Investigation
ASTM E 274-97	Standard Test Method for Skid Resistance of Paved Surfaces Using a Full-Scale Tire
ASTM E 303-93	Standard Test Method for Measuring Surface Frictional Properties Using the British Pendulum Tester
ASTM E 494-95	Standard Practice for Measuring Ultrasonic Velocity in Materials
AASHTO T 24-02	Obtaining and Testing Drilled Cores and Sawed Beams of Concrete
AASHTO T 242-96	Frictional Properties of Paved Surfaces Using a Full-Scale Tire
AASHTO T 260-97	Sampling and Testing for Chloride Ion in Concrete and Concrete Raw Materials
AASHTO T 277-96	Electrical Indication of Concrete's Ability to Resist Chloride Ion Penetration
AASHTO T 278-90	Surface Frictional Properties Using the British Pendulum Tester
SHRP Product 2030	Standard Test Method for Chloride Content in Concrete

APPENDIX B

Guidelines for NBI concrete deck ratings followed by CDOT

Units: Each

Concrete bridge deck: This element defines concrete bridge decks with no surface protection of any type and constructed with uncoated reinforcement. Report the condition state that most nearly represents the entire decks.

Table B.1 Element Condition State of Bridge Decks - NBI

Condition State	Description	Feasible actions
1	No repaired areas No spalls/ Delaminations	• DN • Add a protective system
2	Repaired areas and/or spalls/delaminated areas combined distress of 2% of total deck area or less	• DN • Repair delaminated/Spall areas • Add a protective system
3	Repaired areas and/or spalls/delaminated areas combined distress of 10% or less of total deck area.	• DN • Repair delaminated/Spall areas • Repair spalled areas and add a protective system on entire deck
4	Repaired areas and/or spalls/delaminated areas combined distress of greater than 10% and less than 25% of total deck area.	• DN • Repair delaminated/Spall areas • Repair spalled areas and add a protective system on entire deck
5	Repaired areas and/or spalls/delaminated areas combined distress of more than 25% of total deck area.	• DN • Repair spalled areas and add a protective system on entire deck • Replace deck